JOURNAL OF NEUROGENETICS
https://doi.org/10.1080/01677063.2025.2465536

Taylor & Francis
Taylor & Francis Group

ORIGINAL RESEARCH ARTICLE

OPEN ACCESS Check for updates

Drosophila WDFY3/Bchs overexpression impairs neural function

Marek B. Körner[a,b], Akhil Velluva[a], Linnaeus Bundalian[a], Knut Krohn[c], Kathleen Schön[c], Isabell Schumann[a], Jessica Kromp[a,d], Andreas S. Thum[d], Antje Garten[e], Julia Hentschel[a], Rami Abou Jamra[a], Achmed Mrestani[b,f], Nicole Scholz[b], Tobias Langenhan[b] and Diana Le Duc[a,g1]

[a]Institute of Human Genetics, University of Leipzig Medical Center, Leipzig, Germany; [b]Rudolf Schönheimer Institute of Biochemistry, Division of General Biochemistry, Leipzig University, Leipzig, Germany; [c]Core Unit DNA-Technologies, Medical Faculty, Leipzig University, Leipzig, Germany; [d]Department of Genetics, Institute of Biology, Leipzig University, Leipzig, Germany; [e]Pediatric Research Center, University Hospital for Children and Adolescents, Leipzig University, Leipzig, Germany; [f]Department of Neurology, University of Leipzig Medical Center, Leipzig, Germany; [g]Department of Evolutionary Genetics, Max Planck Institute for Evolutionary Anthropology, Leipzig, Germany

ABSTRACT

Pathogenic variants in *WDFY3*, a gene encoding for an autophagy adaptor termed ALFY, are linked to neurodevelopmental delay and altered brain size in human probands. While the role of *WDFY3* loss-of-function is extensively studied in neurons, little is known about the effects of *WDFY3* upregulation in different cell types of the central nervous system (CNS). We show that overexpression of the *Drosophila melanogaster WDFY3* ortholog, *Bchs*, in either glia or neurons impaired autophagy and locomotion. *Bchs* glial overexpression also increased VNC size and glial nuclei number significantly, whereas neuronal *Bchs* overexpression affected wing and thorax morphology. We identified 79 genes that were differentially expressed and overlapped in flies that overexpress *Bchs* in glial and neuronal cells, respectively. Additionally, upon neuronal *Bchs* overexpression differentially expressed genes clustered in gene ontology categories associated with autophagy and mitochondrial function. Our data indicate that glial as well as neuronal *Bchs* upregulation can have detrimental outcomes on neural function.

ARTICLE HISTORY
Received 21 October 2024
Accepted 6 February 2025

KEYWORDS
WDFY3; *Bchs*; neurodevelopmental delay; transcriptomics; autophagy

1. Introduction

Over the past decade, a growing body of evidence, including functional analyses and patient-related data, has provided substantial support for the involvement of *WDFY3* in neurodevelopmental disorders (Le Duc *et al.*, 2019; Stessman *et al.*, 2017; Wang *et al.*, 2016). *WDFY3* encodes an autophagosomal scaffolding protein involved in targeted recruitment and destruction of macromolecular components including aggregation-prone proteins (Clausen *et al.*, 2010; Filimonenko *et al.*, 2010; Finley *et al.*, 2003; Simonsen *et al.*, 2004).

Previous studies in mice demonstrated that *Wdfy3* regulates neurodevelopmental processes such as neuronal connectivity, proliferation, migration, and synaptic morphology (Dragich *et al.*, 2016; Orosco *et al.*, 2014; Schaaf *et al.*, 2022; Søreng *et al.*, 2022). Loss-of-function variants of *WDFY3* or its *Drosophila* ortholog *blue cheese* (*Bchs*) result in protein aggregation, indicating autophagic defects (Clausen *et al.*, 2010; Filimonenko *et al.*, 2010; Finley *et al.*, 2003; Fox *et al.*, 2020; Han *et al.*, 2015; Hebbar *et al.*, 2015; Lim & Kraut, 2009; Simonsen *et al.*, 2004). Although glial cells are known to play an essential role for neuronal function and neurodevelopment (Bittern *et al.*, 2021; Kim *et al.*, 2020; Lago-Baldaia *et al.*, 2020; Rahman *et al.*, 2022), they have received rather little attention in the effort to unravel *WDFY3*-associated pathomechanisms. So far, it was shown that loss of *Wdfy3* is accompanied by mislocalization of glial guidepost cells, which provide guidance cues for the formation of axonal tracts (Dragich *et al.*, 2016). Further, *Wdfy3* is involved in the turnover of oligodendrocytic myelin sheaths (Aber *et al.*, 2022). Hypomorphic *Wdfy3* alleles also increase symmetric proliferative divisions of radial glial cells, neural stem cells which give rise to neurons and glia (Orosco *et al.*, 2014). Single-cell RNA-seq demonstrated an approximately 10× higher *WDFY3* expression in neurons and glial cells compared to all other cells (nTPM > 200) with oligodendrocytes showing the highest expression (nTPM > 400) (Karlsson *et al.*, 2021). Hence, glial cells may play an important role in the pathophysiology of *WDFY3*-related neurodevelopmental disorders.

Currently, an increasing number of studies concentrate on loss of *WDFY3/Bchs* and its effects on the nervous system with a focus on neuronal impairment. However, little is known about the consequences of *WDFY3* upregulation on the nervous system. Only one individual carrying a copy-number variant covering 18.27 Mb including the whole *WDFY3* gene was reported in the Decipher database (patient-ID 355087) (Firth *et al.*, 2009). This individual

CONTACT Diana Le Duc Gabriela-Diana.LeDuc@medizin.uni-leipzig.de Institute of Human Genetics, University of Leipzig Medical Center, Leipzig, Germany; Marek B. Körner marek.koerner@medizin.uni-leipzig.de Institute of Human Genetics, University of Leipzig Medical Center, Leipzig, Germany
[1]Additional affiliation of Diana Le Duc: Human Genetics Department, Center for Diagnostics GmbH, Chemnitz Clinics.
Supplemental data for this article can be accessed online at https://doi.org/10.1080/01677063.2025.2465536.
© 2025 The Author(s). Published by Informa UK Limited, trading as Taylor & Francis Group
This is an Open Access article distributed under the terms of the Creative Commons Attribution License (http://creativecommons.org/licenses/by/4.0/), which permits unrestricted use, distribution, and reproduction in any medium, provided the original work is properly cited. The terms on which this article has been published allow the posting of the Accepted Manuscript in a repository by the author(s) or with their consent.

presented with attention deficit hyperactivity disorder, autistic behavior, and intellectual disability. In *Drosophila*, it was demonstrated that neuronal *Bchs* overexpression can have detrimental outcomes like impaired synaptic structures, eye morphology, lysosomal vesicle trafficking, and increased larval brain size (Khodosh *et al.*, 2006; Kraut *et al.*, 2001; Kriston-Vizi *et al.*, 2011; Lim & Kraut, 2009; Simonsen *et al.*, 2007). Here, we sought to further characterize the effect of *Bchs* overexpression in different neural cell types, that is, glia and neurons, on the nervous system. While both glial and neuronal *Bchs* overexpression impaired autophagy and locomotion, ventral nerve cord (VNC) size was enlarged only after overexpression in glial cells. Moreover, glial *Bchs* overexpression increased the developmental time. On the other hand, only neuronal *Bchs* overexpression disturbed wing and thorax development. Further, based on transcriptomics analyses we identified differentially expressed genes in glial and neuronal *Bchs* overexpression flies compared to the respective controls. We found an overlap of 79 differentially expressed genes in both *Bchs* overexpression conditions, which may be involved in the pathological mechanism that unfolds upon *WDFY3* dysfunction.

2. Materials and methods

2.1. Fly husbandry

Flies were maintained on standard cornmeal food at 25 °C and a 12:12-light/dark cycle. The following *Drosophila melanogaster* strains were used:

w^{1118}
;; repo-GAL4/TM6B,Tb, (RRID:BDSC_7415)
;; nSyb-GAL4/TM3,Sb, (gift from J. Simpson)
; UAS-bchs::HA, (RRID:BDSC_51636) (in the following abbreviated as *UAS-bchs*)
;; act5C-Gal4/TM6B,Tb,Sb, (RRID:BDSC_3954)
; ok6-GAL4 w^{+}, (Marqués *et al.*, 2002)
; UASp-GFP-mCherry-Atg8a, (RRID:BDSC_37749)
; UAS-mCD8::GFP, UAS-mCD8::GFP, (RRID:BDSC_5137)
;; UAS-mCD8::GFP, (RRID:BDSC_5130)
; Burs-GAL4, (RRID:BDSC_40972)
;; CCAP-GAL4, (RRID:BDSC_25686)
; rL82-GAL4, (Sepp & Auld, 1999)
; nrv2-GAL4, (RRID:BDSC_6800)
;; c527-Gal4, (RRID:BDSC_90391)

2.2. Mendelian ratio and adult developmental time

Fifteen virgin females (*UAS-bchs/Sb^{1}*) and five males (cell type-specific reporter-*Gal4/Sb^{1}*), all carrying the balancer chromosome (marker: *Sb^{1}*), were crossed and switched to a new vial every day. Numbers of flies carrying the balancer chromosome (no *Bchs* overexpression) and flies not carrying the balancer (*Bchs* overexpression) in the F1 generation of five vials were counted for each genotype. Newly hatched flies were counted every 24 h. For each vial, counting was started on the day the first adult fly hatched and continued for 10 days.

2.3. PEDtracker – embryonal developmental time, larval and pupal size

The development of panneuronal *Bchs* overexpression flies (*nSyb-Gal4/UAS-bchs*) as well as the controls *nSyb-Gal4/+* and *UAS-bchs/+* was monitored using the PEDtracker system (Schumann & Triphan, 2020). According to the previously published protocol, the development of *Drosophila* was observed from egg hatching to pupation. Larval hatching timepoint, larval size over development as well as the pupal size were then manually measured using ImageJ (Schneider *et al.*, 2012). Statistical analysis was performed using Kruskal–Wallis test or one-way ANOVA depending on the distribution of the data.

2.4. Assessing the condition of wings and thoraces

Twenty virgin females and 10 males were crossed and switched to a new vial every second day. For each genotype, the F1 generation in three vials was analyzed. For each vial, collecting flies was started on the day the first adult fly hatched and continued for five days. The condition of the wings and thoraces was evaluated 24 h after collecting the flies (24 – 48 h old flies). Wings were categorized into folded, partially folded, and expanded. Thoraces were categorized into dimpled and not dimpled.

2.5. Larval locomotion

Petri dishes with a diameter of 9 cm filled with 1% agarose were prepared. Five third instar larvae were placed in the middle of a petri dish and recorded (camera: Logitech C920 HD Pro) for 1 min. The first 5 s of a recording were dismissed and the larval behavior of the following 30 s investigated. Recordings were analyzed by using the ImageJ freehand line tool to measure the length of the crawled route of a larva. For each genotype, 30 larvae were examined if not stated otherwise.

2.6. Immunohistochemistry

Larvae: Wandering third instar larvae were dissected in ice-cold HL-3 solution (Stewart *et al.*, 1994), fixed with PFA (4% in PBS) and collected in 1× PBS. Blocking, primary antibody incubation and secondary antibody incubation were consecutively performed in PBT (1× PBS + 0.05% Triton X-100, Sigma-Aldrich) containing 5% normal goat serum (NGS, Jackson ImmunoResearch) at 4 °C overnight. Antibody incubation steps were followed by washing two times shortly and three times 15 min (1× PBS + 0.05% Triton X-100). Samples were stored in Vectashield (Vector Laboratories, H-1000) at 4 °C overnight before mounting. For mounting of larval central nervous systems (CNS), reinforcement rings (Herma, #5898) were adhered on slides, 5 µl of Vectashield added to the middle of each ring and up to five larval CNS placed into each ring with the dorsal side up.

Adult flies: The CNS of adult female flies (21 – 33 h old) were dissected in ice-cold Ringer solution, fixed in 4% PFA

for 30 min at room temperature and collected in 1× PBS. Blocking was done at room temperature for 24 h in PBT (1× PBS + 1% Triton X-100) containing 5% NGS. Primary antibody incubation was carried out at 4 °C for 24 h and secondary antibody incubation at 4 °C for 24 – 48 h. Antibody incubation steps were followed by moving samples to room temperature for 1 h and washing two times shortly and three times 15 min with PBT. Samples were stored in Vectashield at 4 °C overnight before mounting. For mounting, two reinforcement rings (Herma, #5898) were adhered on top of each other on a slide to reduce compression of the tissue, 5 µl of Vectashield added and up to five CNS placed into the middle with the anterior side up.

The following antibodies were used at following dilutions: rabbit-anti-Ref(2)P (1:500, Abcam, ab178440), mouse-anti-repo (1:250, DSHB, 8D12 concentrate), mouse-anti-even skipped (1:50, DSHB, 3C10), goat-anti-mouse conjugated with Alexa Fluor-488 or –405 (1:250, Invitrogen, A-11001, RRID: AB_2534069 and A-31553, RRID: AB_221604), goat-anti-horseradish peroxidase (HRP) conjugated with Alexa Fluor-488 or –647 (1:250, Jackson ImmunoResearch, 123–545-021, RRID: AB_2338965 and 123–605-021, RRID: AB_2338967), Cy3- or Cy5-conjugated goat-anti-rabbit (1:250, Jackson ImmunoResearch, 111–165-144, RRID:AB_2338006 and 111–175-144, RRID: AB_2338013).

2.7. Central nervous system size measurement

Larval VNC length was measured and normalized to the larval length which was determined before dissection. Larvae were placed into a petri dish filled with HL-3 on ice and imaged (camera: Leica DFC365 FX, microscope: Leica MZ10 F). Brains were stained against HRP, imaged and a maximum projection of the z-stack was performed with ImageJ. The length of the larvae and the VNC including the subesophageal zone were measured with the ImageJ Straight Line tool.

The size of the VNC of adult flies was determined and normalized to the fly length. The adult fly was anesthetized by putting it in a vial on ice. The fly was transferred to a petri dish and imaged (camera: Leica DFC365 FX, microscope: Leica MZ10 F). The central nervous system was stained against HRP, imaged, and a maximum projection was performed. Lengths of the fly and the VNC were measured with the ImageJ Straight Line tool.

2.8. Number of glial nuclei

Larvae were stained with anti-repo antibody and imaged. Repo-positive nuclei were counted using the ImageJ plugin cell counter. For the analysis of glial nuclei number in the peripheral nervous system, glial nuclei number was determined at the entry point of the peripheral nerve bundle into the body wall muscles at the region, where the bundle divides into the TN, ISN, and SN nerve branches. Peripheral nerves innervating the hemisegments A4R and A4L were analyzed.

2.9. Colocalization of GFP-mCherry-Atg8 fluorophore signals

Larval brains were dissected and fixed as described before. Brains were stored in Vectashield for at least 24 h. Brains were imaged as described before. Images were deconvoluted using Huygens Essentials software (strategy: standard). Analyses of images were performed with the ImageJ plugin coloc 2 (Pearson correlation, above threshold) and using the freehand selection tool to set a ROI surrounding the brain.

2.10. Imaging

Image acquisition was performed with a Leica SP8 confocal microscope unless specified otherwise.

2.11. RNA extraction and sequencing

RNA was extracted from five female and five male fly heads for one sample. Flies (22 – 31 h after eclosion) were anesthetized with carbon dioxide and heads were cut using a scalpel. Heads were immediately transferred to an ice-cold 2-ml Eppendorf tube containing Trizol or RLT buffer. RNA extraction followed immediately using the RNeasy Micro Kit (Qiagen, Cat. No. 74004) according to protocol or exchanging the first step of homogenization in RLT buffer with the following Trizol protocol (Invitrogen, Cat. No. 15596026). Heads were homogenized in 500 µl Trizol, centrifuged for 5 min at 10,000 rpm at 4 °C, supernatant was transferred to a new tube, 200 µl chloroform (Carl Roth, No. 6340.1) was added and the tube was shaken for 15 s. An incubation step at room temperature for 3 min was followed by centrifugation for 5 min at 10,000 rpm at 4 °C. The upper aqueous phase was transferred in a new tube and it was continued with the RNeasy Micro Kit protocol. Homogenization was performed on ice using the Ultra-Turrax (IKA T10 basic) five times for 10 s. For each genotype, five samples were sequenced.

RNA sequencing (RNA-seq) libraries were prepared using TruSeq RNA Library Prep Kit v2 (Illumina, San Diego, CA) and sequenced on an Illumina NovaSeq platform with 151 bp paired-end reads with an average of ~135 million reads per library.

2.12. Differential gene expression analysis

RNA-Seq reads were mapped to the *Drosophila* genome assembly BDGP6.32 (GCA_000001215.4) with STAR (version 2.6.1d) (Dobin *et al.*, 2013). Reads were processed as previously described (Körner *et al.*, 2022). We computed the transcript levels with htseq-count (version 0.6.0) (Anders *et al.*, 2015). Genes with a sum of less than 10 reads in all samples together were excluded from further analysis. Differential expression of genes was determined with the R package DESeq2 (version 1.30.1) (Love *et al.*, 2014), which uses the Benjamini–Hochberg method to correct for multiple testing (Benjamini *et al.*, 2001). Genes were considered to be significantly differentially expressed if p-adj < 0.05. To

check clustering of RNA-sequencing samples of subjects and controls, a principal component analysis (PCA) was performed with the R package pcaExplorer (version 2.6.0) (Marini & Binder, 2019). RNA count data were variance stabilized transformed and the 500 most variant genes (top n genes) were selected for computing the principal components. We tested five samples of adult heads from glial/neuronal *Bchs* overexpression (*repo-Gal4/UAS-bchs* and *nSyb-Gal4/UAS-bchs*, respectively) against the pooled samples of both controls, five samples of the *Gal4*-driver control (*repo-Gal4/+* and *nSyb-Gal4/+*, respectively) and five samples of the *UAS* control (*UAS-bchs/+*).

To identify which pathways are enriched with differentially expressed genes, we used the clusterProfiler 4.0 package with a hypergeometric test and the *Drosophila* GO annotations org.Dm.eg.db v.3.18 (Carlson, 2019; Wu *et al.*, 2021). For visualization of enriched GO terms, the package enrichplot was utilized (Yu, 2018).

2.13. Statistics

Data are shown as mean ± SEM. Statistical analyses were performed with SigmaPlot 12.5 (Systat software) using two-tailed unpaired Student's *t*-tests, if not stated otherwise. Mann–Whitney Rank Sum tests were performed for non-normally distributed data (Shapiro–Wilk test) and data that failed the Equal Variance test.

3. Results

3.1. Developmental delay in glial Bchs overexpression flies

In flies, both loss-of-function and overexpression of the *WDFY3* ortholog *Bchs* were previously shown to impair neuronal function (Finley *et al.*, 2003; Hebbar *et al.*, 2015; Khodosh *et al.*, 2006; Kraut *et al.*, 2001; Kriston-Vizi *et al.*, 2011; Lim & Kraut, 2009; Sim *et al.*, 2019; Stessman *et al.*, 2017). To better understand the relevance of *Bchs* in different neural cell types, we tested the effect of *Bchs* overexpression in glial cells (*repo-Gal4*) and neurons (*nSyb-Gal4*) on development, locomotion, VNC morphology, and autophagy (DiAntonio *et al.*, 1993; Sepp *et al.*, 2001). We found that panglial *Bchs* overexpression delayed the development from egg to adult fly (Figure 1(A)). Importantly, Mendelian ratios of the adult F1 generation of crossing *Gal4/Sb* with *UAS-bchs/Sb* for panglial and panneuronal *Bchs* overexpression corresponded to the expected ratios, but ubiquitous *Bchs* overexpression (*act5C-Gal4*) was lethal (Figure S1). The developmental time of neuronal *Bchs* overexpression animals was further investigated to exclude a delay in early developmental steps, which cannot be detected at the stage of adult eclosion. The timepoint of larval hatching was not delayed in animals overexpressing *Bchs* in neurons indicating normal embryonal development (Figure S2A). However, a significantly reduced size of neuronal *Bchs*-overexpressing larvae was observed in early larval development (62.44 h and 100.8 h after egg laying), but not in later larval stages (153 h after egg laying) (Figure S2B). These data suggest that neuronal *Bchs* overexpression causes changes in development during early larval stages.

Further, we observed pronounced malformations of the wings and thorax in flies overexpressing *Bchs* panneuronally (Figure 1(B,E)). Adult flies did not properly expand their wings (~90%) and displayed a dimpled dorsal anterior thorax (~43%). In contrast, only a small percentage of flies overexpressing *Bchs* in glial cells (wing: ~22%, thorax: 3%) presented with those deficits (Figure 1(D,E)). Crustacean cardioactive peptide (CCAP) neurons are known to play an essential role in wing expansion (Luan *et al.*, 2006; Park *et al.*, 2003). Therefore, we hypothesized that *Bchs* overexpression in this subtype of neurons caused the wing and thorax abnormalities. Driving *Bchs* overexpression specifically only in CCAP neurons (*CCAP-Gal4*) resulted in almost complete penetrance of those defects (wing: ~100%, thorax: ~99%), as opposed to *Bchs* overexpression in motoneurons (*ok6-Gal4*, wing: ~19%, thorax: ~1%)) (Figure S3). Similarly, utilizing *burs-Gal4*, which drives expression in many CCAP neurons, provoked wing and thorax impairments in ~99% and ~49% of flies, respectively (Figure S3) (Luan *et al.*, 2006; Peabody *et al.*, 2008). Hence, CCAP neurons are sensitive to *Bchs* overexpression.

3.2. Bchs overexpression leads to altered transcriptome profiles

To understand which molecular pathways are affected by *Bchs* overexpression and how this impacts brain function, we performed RNA-seq on heads from adult flies overexpressing *Bchs* in glia or neurons. It is important to note that whole heads were analyzed to be able to also detect cell non-autonomous changes. *Bchs* displayed a higher upregulation in fly heads with glial than neuronal-driven overexpression (Figure 2(A), Table S1, 2, 7.39-fold vs. 4.45-fold higher expression). We identified more differentially expressed genes (i.e. genes with different expression in *Bchs* overexpression flies as opposed to control animals carrying only the *Gal4* driver or only the *UAS*-target gene) in the panneuronal *nSyb-Gal4/UAS-bchs* condition (2,107 genes) than in the glial *Bchs* overexpression heads (156 genes) (Table S1, 2, Figure S4). For glial *Bchs* overexpression, GO categories related to cell junctions including septate junctions were enriched (Table S4). Whereas, neuronal *Bchs* overexpression led to an over-representation of GO categories most prominently related to mitochondria but also to many other processes and components, for example, autophagy (Figure 2(D), Table S5). Seventy-nine genes were similarly differentially expressed upon *Bchs* overexpression in glia and neurons, which represented a highly significant overlap (p values < 0.0001 from 1,000 simulations using 13,000 genes for random sampling) (Figure 2(B), Table S3). Expression of 73 of these genes was dysregulated in the same direction in glial and neuronal *Bchs* overexpression flies.

Among the overlapping differentially expressed genes we identified *Iml1* and *Rab32* (Table S3), which are known to play an important role in autophagy (Hirota & Tanaka, 2009; Wang *et al.*, 2012; Wu & Tu, 2011), which is the main known function of *WDFY3*/*Bchs* (Clausen *et al.*, 2010;

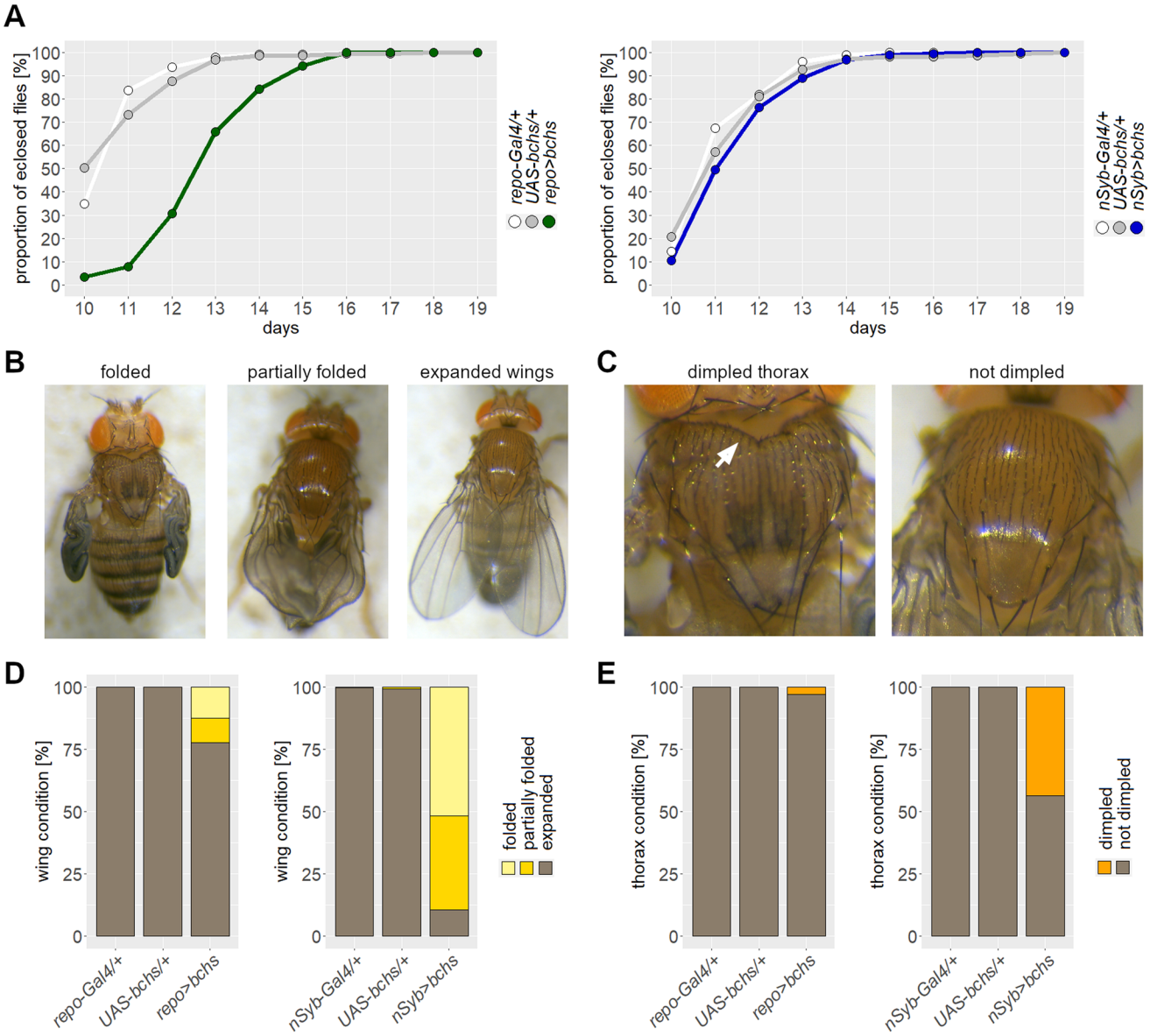

Figure 1. Developmental deficits in Bchs overexpression flies. (A) Glial *Bchs* overexpression (left, *repo > bchs*, green, $n = 88$) prolonged the developmental time from egg to eclosion of adult flies, unlike neuronal overexpression (right, *nSyb > bchs*, blue, $n = 190$), in comparison to controls (left: *repo-Gal4/+* white, $n = 140$, *UAS-bchs/+* gray, $n = 153$) (right: *nSyb-Gal4/+* white, $n = 104$, *UAS-bchs/+* gray, $n = 164$). Flies of 5 vials were pooled. (B,C) Images of flies overexpressing *Bchs* in neurons. *Bchs* overexpression caused wing expansion and dimpled thorax defects (arrow). (D,E) Quantification of wing (D) and thorax (E) defects. Both defects had a higher rate in neuronal ($n = 391$) than in glial *Bchs* overexpression ($n = 72$). left: *repo-Gal4/+*, $n = 211$; *UAS-bchs/+*, $n = 491$. right: *nSyb-Gal4/+*, $n = 434$; *UAS-bchs/+*, $n = 324$.

Filimonenko *et al.*, 2010; Finley *et al.*, 2003; Simonsen *et al.*, 2004). For neuronal and glial *Bchs* overexpression, 51 and three of the differentially expressed genes, respectively, are annotated to the GO category autophagy (GO:0006914) (Figure 2(C)). Moreover, *Tau*, which is strongly linked to neurodegenerative diseases, was upregulated (Table S2, 1.2-fold higher expression, *adj-p* = 0.003) in flies overexpressing *Bchs* panneuronally (Gao *et al.*, 2018; Goedert *et al.*, 2024).

Genes of which dysregulations were previously associated with the combination of unexpanded wings and a dimpled thorax, namely *TBPH*, *Gclc*, and *EndoU*, were not differentially expressed in *Bchs* overexpression flies (Laneve *et al.*, 2017; Mercer *et al.*, 2016; Vanden Broeck *et al.*, 2013). However, *Pburs*, encoding a subunit of the hormone bursicon which is necessary for wing expansion (Dewey *et al.*, 2004; Lahr *et al.*, 2012; Loveall & Deitcher, 2010; Luo *et al.*, 2005), was significantly upregulated in panneuronal *Bchs* overexpression flies (Table S2, 10-fold higher expression, *adj-p* = 0.0008). Taken together, there was a significant number of overlapping genes that suffered dysregulation after *Bchs* overexpression in neurons or glial cells. This implies an altered molecular mechanism regardless of the inquired cell type.

3.3. Bchs overexpression causes ref(2)P accumulation

The previously shown involvement of *WDFY3/Bchs* in autophagy directed us to examine the effect of *Bchs* overexpression on the autophagic process (Clausen *et al.*, 2010;

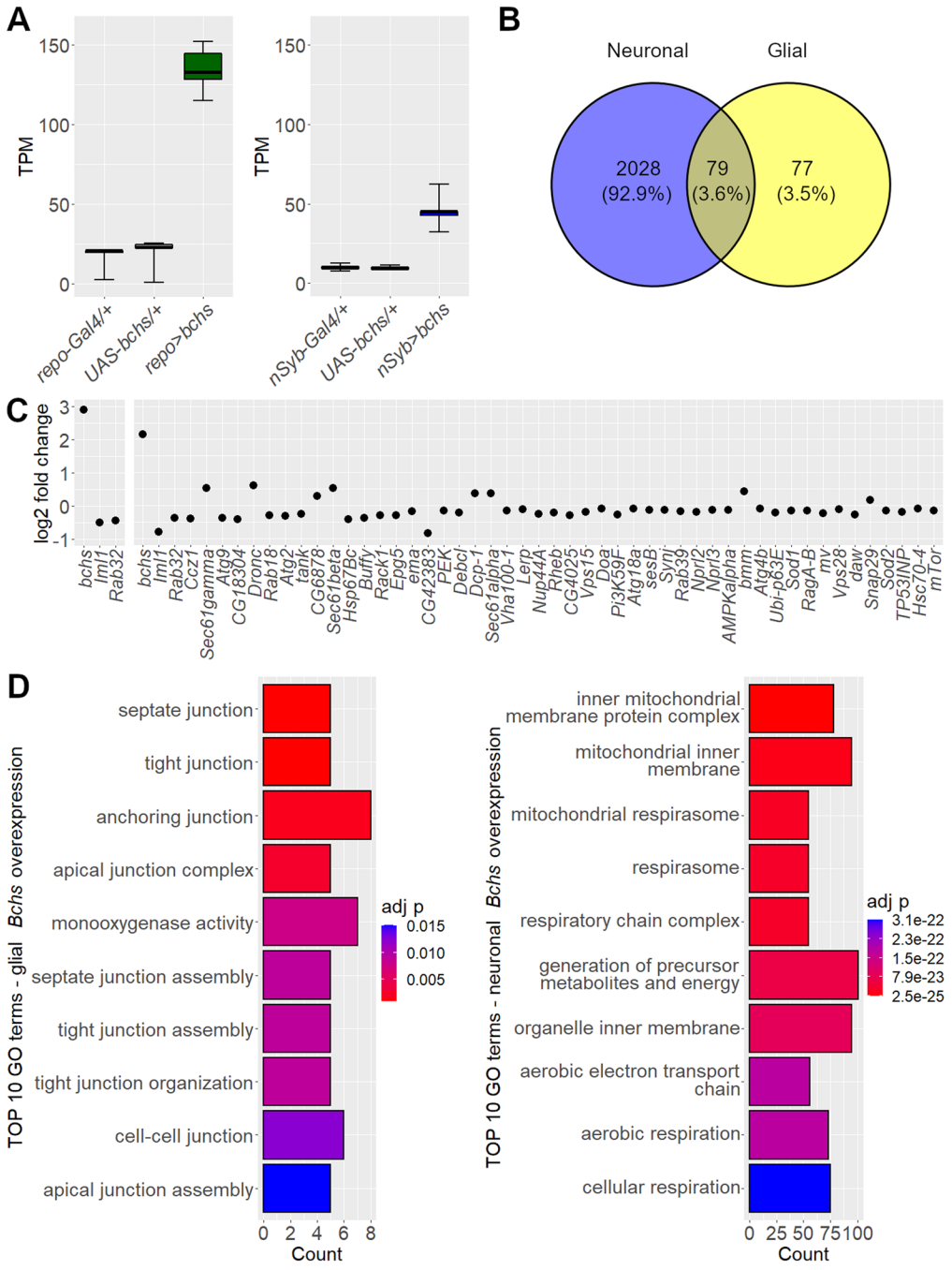

Figure 2. Differential gene expression in Bchs overexpression flies**.** (A) Expression levels of *Bchs* transcripts in glial *Bchs* overexpression flies (left, green, *repo > bchs*), neuronal *Bchs* overexpression flies (right, blue, *nSyb > bchs*), and controls. white: *repo-Gal4/+* or *nSyb-Gal4/+*, gray: *UAS-bchs/+*. $n = 5$. TPM: transcripts per million. Horizontal line represents the median. Lower and upper hinges correspond to the 25th and 75th percentiles. Whiskers show maximum and minimum values. (B) Venn diagram displaying the number of differentially expressed genes in neuronal *Bchs* overexpression flies (left, blue) and glial *Bchs* overexpression flies (right, yellow). (C) Differentially expressed genes in glial (left) and neuronal (right) *Bchs* overexpression flies that are associated with autophagy (GO:0006914) are displayed and plotted against their log2-fold change. (D) GO enrichment analysis. Displayed are the top 10 GO terms enriched in differentially expressed genes of glial (left) and neuronal (right) *Bchs* overexpression flies, respectively. The count specifies the number of differentially expressed genes related to the GO term.

Filimonenko *et al.*, 2010; Finley *et al.*, 2003; Napoli *et al.*, 2018, 2021; Simonsen *et al.*, 2004). The autophagy adaptor ref(2)P links ubiquitinated proteins to autophagosomes *via* interactions with Atg8a, which is anchored to autophagic compartment membranes (Jain *et al.*, 2015). Aggregates of ref(2)P are considered as a marker of misfunctioning protein degradation by autophagy or the ubiquitin-proteasome system (UPS) (Bartlett *et al.*, 2011; Nezis *et al.*, 2008; Pircs *et al.*, 2012). *Bchs* loss-of-function variants have been described to lead to a ref(2)P (human homolog: p62) accumulation and an increase in early autophagic compartments, suggesting an impaired autophagic flux (Clausen *et al.*, 2010; Hebbar *et al.*, 2015; Sim *et al.*, 2019). To test whether *Bchs* overexpression impairs autophagy, ref(2)P immunostainings and an autophagic vesicle pH-reporter were utilized. Our data indicate strong accumulation of ref(2)P in the thoracic neuromeres of the VNC and milder also in the brain upon glial *Bchs* overexpression in the adult CNS (Figure 3(B)).

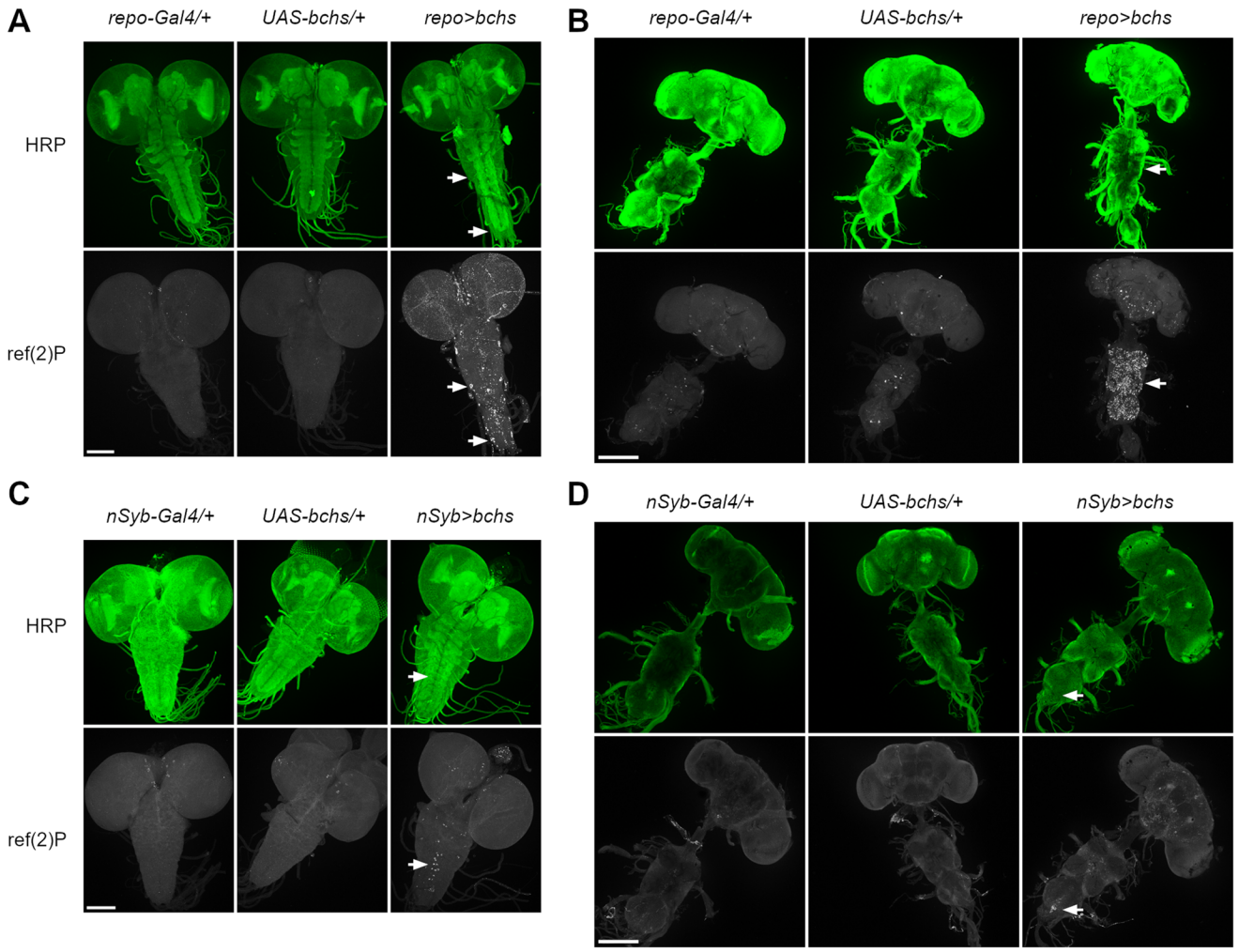

Figure 3. Bchs overexpression provoked ref(2)P accumulation. (A–D) CNS were stained against HRP (top), a neuronal marker, and ref(2)P (bottom), a component of protein aggregates. Arrows indicate ref(2)P signals. (A,B) Glial *Bchs* overexpression (*repo > bchs,* right) caused widely spread accumulation of ref(2)P in larval (A) and adult (B) CNS compared to controls (*UAS-bchs/+*, middle and *repo-Gal4/+*, left). Strong ref(2)P staining was displayed in the thoracic neuromeres of the adult VNC. C, D) Neuronal *Bchs* overexpression (*nSyb > bchs,* right) caused ref(2)P accumulation in the larval VNC (C) and in the adult CNS in the brain and posterior region of the VNC (D). Controls: *UAS-bchs/+*, middle and *nSyb-Gal4/+*, left). A, C) Scale bar: 100 µm. B, D) Scale bar: 200 µm.

Consistently, the overall larval CNS showed increased ref(2)P staining (Figure 3(A)).

In contrast, adult flies overexpressing *Bchs* panneuronally accumulated ref(2)P most prominently in the posterior region of the VNC but also with a lower signal intensity in the brain (Figure 3(D)). Larvae displayed ref(2)P aggregates in a subset of neurons in the VNC (Figure 3(C)), which we speculated to be motoneurons due to the location of the cells. Driving *Bchs* overexpression in motoneurons simultaneously with a membrane-bound GFP demonstrated that a subset of motoneurons did form ref(2)P aggregates in response to *Bchs* overexpression (Figure S5). Importantly, overexpression of GFP alone in motoneurons did not provoke accumulation of ref(2)P demonstrating that this is a specific effect of *Bchs* overexpression and not due to general toxicity of overexpression models. It was previously shown that *Bchs* overexpression in *even-skipped* (eve)-positive motoneurons aCC and RP2 leads to morphological abnormalities and neuronal death (Hebbar *et al.*, 2015; Lim & Kraut, 2009; Sim *et al.*, 2019). We thus hypothesized that the ref(2)P signal might localize to eve-positive neurons and conducted a double immunostaining of eve and ref(2)P confirming that a small subset of eve-positive neurons accumulate ref(2)P (Figure S6). However, also eve-negative neurons showed ref(2)P expression.

To further confirm the autophagic defect, we applied a GFP-mCherry-Atg8a reporter to check the ratio of non-acidic to acidic autophagic vesicles in larval brains (Nezis *et al.*, 2010). Fusion of an autophagosome with an endosome or lysosome results in an acidic autophagic vesicle, termed amphisome or autolysosome, respectively. GFP fluorescence is quenched in the acidic environment leading to an mCherry-only signal that does not colocalize with a GFP signal. In larvae overexpressing *Bchs* in glial cells, a significantly increased colocalization of mCherry and GFP signals was observed in comparison to the control indicating a shift of the ratio towards non-acidic autophagic vesicles (Figure 4(A,B,C), S7A). Although whole larval CNS were analyzed, we speculate that the fluorophore spots detected outside the somata mainly drive the enhanced colocalization. Notably, in glial *Bchs* overexpression larvae those spots appeared to be mostly positive for both, GFP and mCherry, whereas the

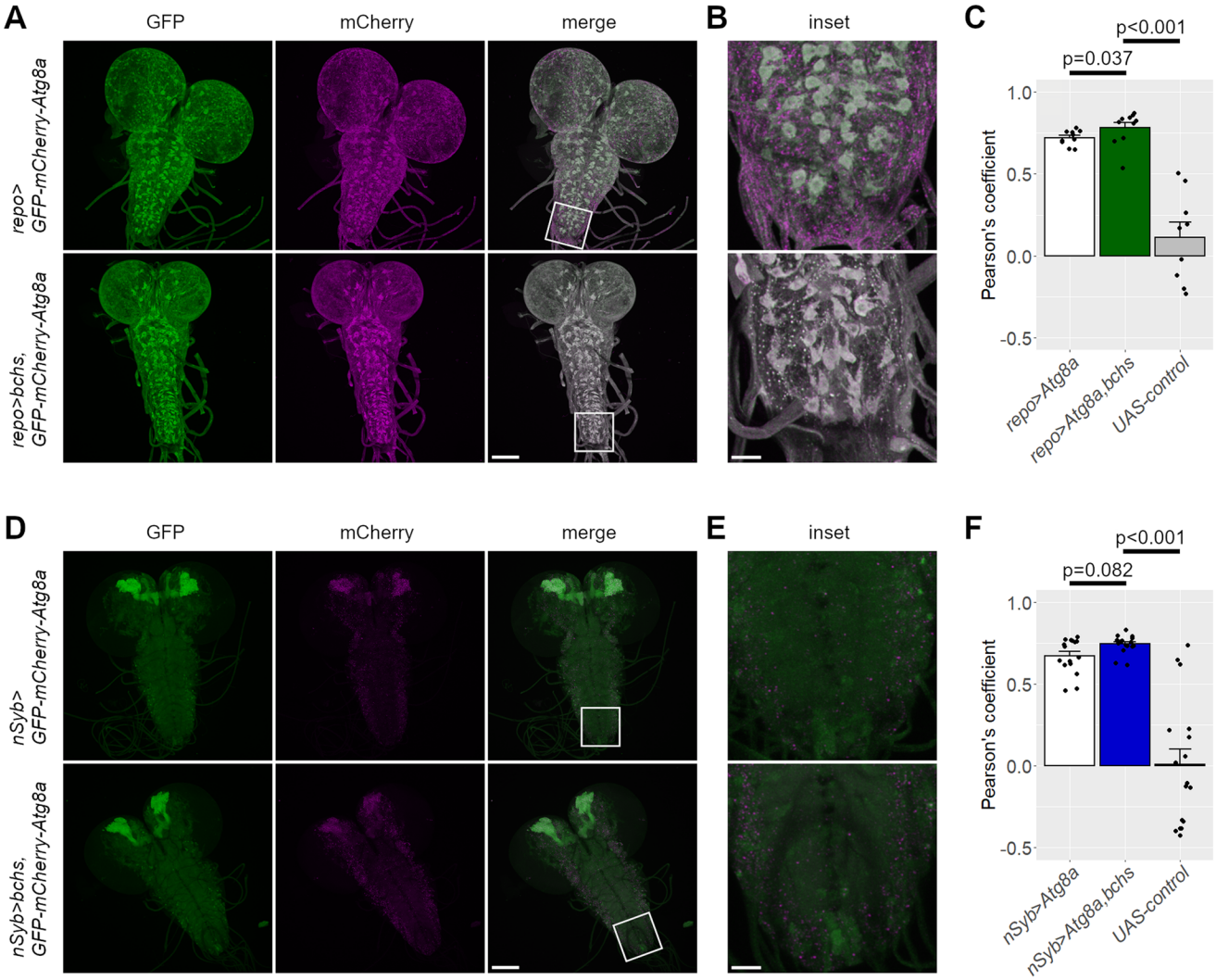

Figure 4. Ratio of non-acidic to acidic autophagic vesicles was shifted to non-acidicity through glial Bchs overexpression. (A – F) The GFP-mCherry-Atg8a reporter was used to investigate autophagic flux in larval brains and was expressed in the same cell type as the *Bchs* overexpression. Autophagic flux was compared between larvae only expressing the Atg8a reporter (top, white, A – C: repo>*GFP-mCherry-Atg8a* and D – F: nSyb>*GFP-mCherry-Atg8a*, abbreviated as *repo > Atg8a* in C and *nSyb > Atg8a* in D) and larvae expressing the Atg8a reporter simultaneously with the *Bchs* overexpression (A – C: bottom, green, repo > bchs, *GFP-mCherry-Atg8a* and D – F: bottom, blue, nSyb > bchs, *GFP-mCherry-Atg8a*). As negative controls animals were used which carried both *UAS*-target genes, but not the *Gal4* (C, F: gray, *UAS-GFP-mCherry-Atg8a/+; UAS-bchs/+*, abbreviated as UAS-control, Figure S6). (A,D) GFP (left) and mCherry (middle) signals were imaged and deconvoluted. Right: GFP and mCherry images merged. Scale bar: 100 µm. Box indicates the region of the insets shown in (B) and (E). (B, E) Scale bar: 20 µm. (C, F) Quantification of colocalization of GFP and mCherry signals using Pearson's coefficient. Statistical comparisons were performed using Mann-Whitney Rank Sum tests. (C) $n \geq 9$. (F) $n \geq 16$. Data are shown as mean ± SEM.

spots were predominantly solely mCherry-positive in the control. Dissimilarly, in animals with panneuronal *Bchs* overexpression no significant difference in the acidic environment of autophagic vesicles was detected (Figure 4(D,E,F), S7B), which might be caused by a less pronounced *Bchs* overexpression using the neuronal *Gal4*-driver than the glial driver (Figure 2(A)). Collectively, the ref(2)P accumulation and change in autophagic compartment acidity indicates that glial *Bchs* overexpression affects autophagic flux prior to or at the step of acidification of autophagic vesicles.

3.2. Glial Bchs regulates VNC size and glial nuclei number

Performing the immunostainings, we noticed a prominent abnormal length of the VNC in glial *Bchs* overexpression animals. Quantification of the VNC size revealed a significant increase of the longitudinal VNC length in larvae and adult flies overexpressing *Bchs* in glia (Figure 5(A,B), S8). In adults, the length of the abdominal but not thoracic neuromeres of the VNC was elongated (Fig S8C). Further, during dissection, the VNC of glial *Bchs* overexpression adult flies seemed to be more fragile and to tear apart more easily than in controls. However, the tissue fragility was not further investigated. In contrast, neuronal *Bchs* overexpression did not alter the VNC length in larvae or adults (Figure 5(A,B)).

We then sought to identify the glial cell type responsible for VNC elongation by enforcing *Bchs* overexpression in glial subtypes through specific *Gal4* drivers. We found that *Bchs* overexpression in subperineural glial cells (*rL82-Gal4*) was sufficient to increase the larval VNC length, while overexpression in perineural (*c527-Gal4*) or wrapping glia (*nrv2-Gal4*) was not (Figure S9). Subperineural glial cells are essential for the blood–brain barrier (BBB) and form septate

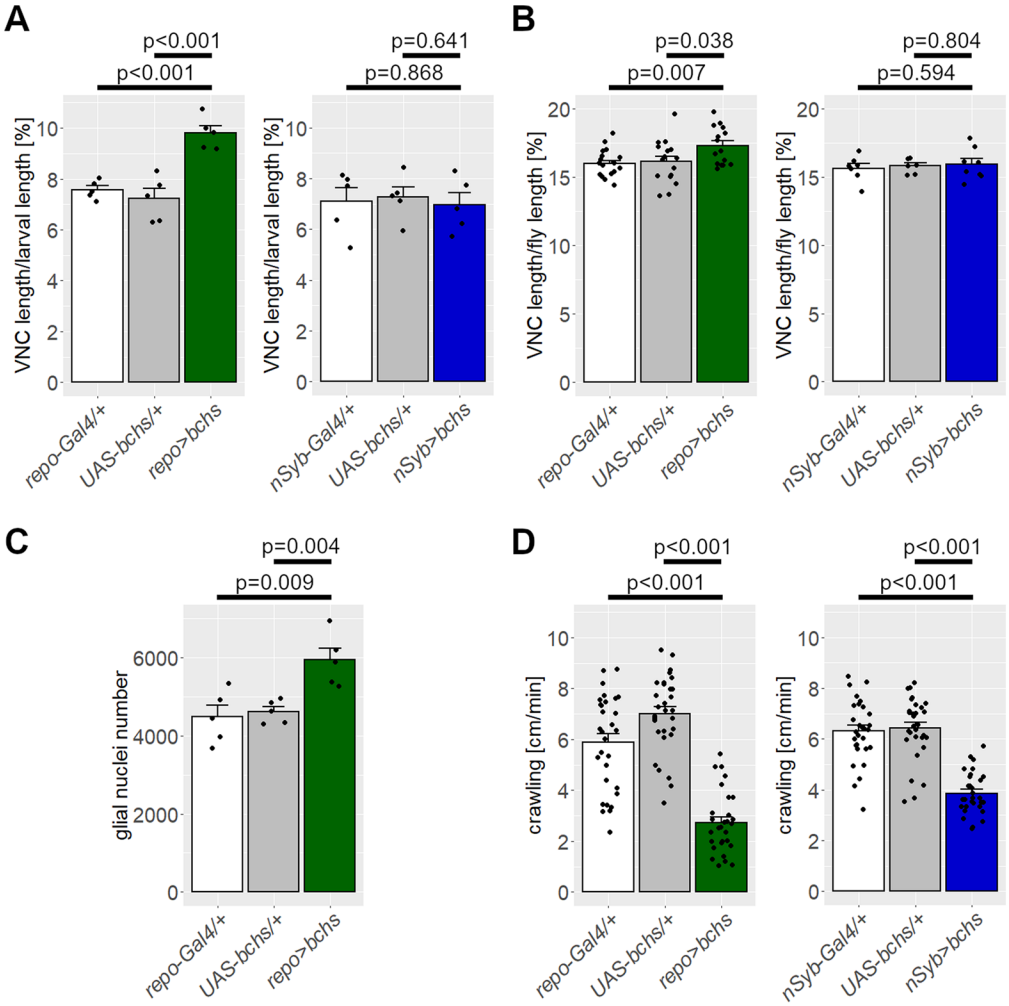

Figure 5. VNC length was elongated by glial Bchs overexpression. (A) Quantification of larval VNC length normalized to the larval length. Increased VNC length was observed in glial *Bchs* overexpression (left, green, *repo > bchs*) larvae but not neuronal overexpression (right, blue, *nSyb > bchs*). $n = 5$. (B) Quantification of adult VNC length normalized to the fly length. Overexpression of *Bchs* in glial cells (left, green, $n \geq 15$), but not in neurons (right, blue, $n \geq 6$), elongated the VNC length. (C) Glial nuclei in the larval CNS were counted by staining against repo. Glial *Bchs* overexpression raised the glial nuclei number. $n = 5$. (D) Overexpression of *Bchs* in glial cells (left, green) or neurons (right, blue) reduced the crawled distance in a given time. $n > 29$. (A–D) Controls: *UAS-bchs/+* (gray) and *repo-Gal4/+* or *nSyb-Gal4/+* (white), respectively. Mann-Whitney Rank Sum tests were performed for statistical comparison of adult VNC length/fly length$_{UAS\text{-}bchs/+ \text{ vs } repo>bchs}$ (B) and crawling$_{repo\text{-}Gal4/+ \text{ vs } repo>bchs}$ (D). All other comparisons were done with Student's t-tests. Data are shown as mean ± SEM.

junctions (Baumgartner *et al.*, 1996; Stork *et al.*, 2008). These data demonstrate that glial *Bchs* plays a role in regulating the CNS morphology.

Elongation of the VNC may be caused by an increased number of glial cells. Therefore, we quantified the number of glial nuclei in the larval CNS using an anti-repo antibody, which is a panglial cell marker (Xiong *et al.*, 1994). Panglial *Bchs* overexpression significantly increased the number of repo$^+$ nuclei in the total CNS but not their density (Figure 5(C), S8D). Considering repo$^+$ nuclei in the VNC and the brain lobes, separately, revealed a gain of nuclei in both regions (Figure S8D). We additionally observed an increased number of glial nuclei in the peripheral nervous system (Figure S10). In conclusion, *Bchs* overexpression can act on glial nuclei number inside and outside the CNS.

Since the VNC is involved in *Drosophila* locomotion behavior (Berni *et al.*, 2012; Gowda *et al.*, 2021; Pulver *et al.*, 2015), the abnormal VNC morphology in glial *Bchs* overexpression animals and the ref(2)P accumulation in the VNC observed in both overexpression conditions, prompted us to test larval crawling. Both panglial and panneuronal *Bchs* overexpression decreased larval crawling velocities indicating a locomotion deficit (Figure 5(D)). Importantly, larval length was not altered by glial or neuronal *Bchs* overexpression implying that crawling velocity was not diminished due to reduced animal size (data not shown). Overexpressing *Bchs* only in the subset of motoneurons (*ok6-Gal4*) was sufficient to slow larval movement (Figure S5C). Notable, phenotypical abnormalities in the peripheral nervous system, which were not investigated in the present study, could also be the underlying cause of the crawling deficit. This is supported by previous studies reporting that neuronal *Bchs* overexpression disturbs the morphology of larval motoneurons and the structure of neuromuscular junctions (Kraut *et al.*, 2001; Lim & Kraut, 2009). To conclude, glial *Bchs* overexpression increased VNC length and glial nuclei number. Additionally, both, glial and neuronal *Bchs* overexpression led to a locomotion deficit.

4. Discussion

Neuronal *Bchs* overexpression was previously demonstrated to impact synaptic morphology, eye morphology, and larval CNS size (Khodosh *et al.,* 2006; Kraut *et al.,* 2001; Kriston-Vizi *et al.*, 2011; Lim & Kraut, 2009; Simonsen *et al.,* 2007). Here, we further characterized the phenotypic outcomes of *Bchs* overexpression. Ubiquitous *Bchs* overexpression was lethal (Figure S1), suggesting that *Bchs* expression levels are highly relevant also in non-neural tissues. We then overexpressed *Bchs* in different cell types of the nervous system to understand how dysregulation in different cells impacts neural function. The present study indicates that besides neuronal also glial *Bchs* overexpression can be detrimental.

4.1. Neuronal Bchs overexpression impairs wing and thorax development

We detected a prolonged developmental time for flies overexpressing *Bchs* in glial cells, but not for panneuronal overexpression, indicating a role of glial *Bchs* for developmental processes (Figure 1(A)). On the other side, neuronal *Bchs* overexpression caused higher rates of wing and thorax defects (Figure 1(D,E)). Driving *Bchs* overexpression only in CCAP neurons was sufficient to cause these morphological phenotypes, implicating that CCAP neurons are involved in the pathomechanism which provokes wing and thorax abnormalities (Figure S3). However, we cannot exclude the additional involvement of other neurons in the observed phenotype. CCAP neurons are well known to have a major role in postecdysis development (Luan *et al.,* 2006; Park *et al.,* 2003). Suppressing their activity disrupts tonic abdominal contractions and air swallowing, a motor program necessary to pump hemolymph into wings to unfold them (Peabody *et al.,* 2009). Further, CCAP neurons secrete the hormone bursicon, required for wing expansion and tanning, into the hemolymph (Dewey *et al.,* 2004; Loveall & Deitcher, 2010; Luo *et al.,* 2005). Interestingly, similar wing and thorax abnormalities were noticed upon misexpression of *TBPH* or knockdown of *Gclc* in CCAP neurons (Mercer *et al.,* 2016; Vanden Broeck *et al.,* 2013). The human ortholog of *TBPH* is *TDP-43*, an RNA-binding protein associated with amyotrophic lateral sclerosis and frontotemporal dementia (Arai *et al.*, 2006; Kabashi *et al.*, 2008; Neumann *et al.*, 2006). Knockdown or overexpression of *TBPH* reduced the number of CCAP neurons in the late pupal and young adult phase (Vanden Broeck *et al.*, 2013). Rescuing the CCAP neuron number through overexpression of the apoptosis inhibitor p35 also rescued the wing and thorax defects. Similarly, a premature degeneration of CCAP neurons was hypothesized to induce the wing and thorax defects in flies depleted of *Gclc*, which is involved in glutathione synthesis (Mercer *et al.,* 2016). Therefore, we suspect that also *Bchs* overexpression might have contributed to a degeneration of CCAP neurons. Importantly, WDFY3 is involved in the removal of mutant TDP-43 (Han *et al.,* 2015), suggesting that *Bchs* overexpression might lead to a misregulation of TBPH in CCAP neurons which induces the wings misfolding and thorax malformations. In our transcriptomic analyses, we did not identify *TBPH* or *Gclc* to be differentially expressed in flies overexpressing *Bchs* in neurons. However, protein levels do not necessarily correlate with mRNA levels. Hence, *Bchs* overexpression could affect the translation of *TBPH* and *Gclc* mRNA or provoke other post-transcriptional effects on TBPH and Gclc, e.g. impacting their degradation. Moreover, performing RNAseq from whole heads might not detect genes which are only differentially expressed in a small subset of cells. On the other side, *Pburs*, a subunit of the hormone bursicon was upregulated (Table S2) (Luo *et al.*, 2005). Null mutants of *Pburs* were similarly described to have a wing expansion deficit (Lahr *et al.,* 2012). The observed weak penetrance of the wing and thorax abnormalities in glial *Bchs* overexpression flies may indicate that in a small number of flies glial *Bchs* overexpression provoked a misfunctioning of CCAP neurons (Figure 1(D,E)). Similarly, the weak penetrance of abnormalities in motoneuronal *Bchs* overexpression could be explained by its expression in CCAP motoneurons but not in CCAP interneurons (Figure S3). To sum up, while glial *Bchs* overexpression affects developmental time, neuronal *Bchs* overexpression impacts wing and thorax development.

4.2. Bchs overexpression impairs autophagic flux

Bchs is an adaptor between ref(2)P and the autophagosomal membrane, therefore, a gain of *Bchs* could be assumed to increase autophagic flux (Clausen *et al.*, 2010; Filimonenko *et al.*, 2010; Sim *et al.*, 2019; Simonsen *et al.,* 2004). However, our data showing ref(2)P aggregation and a shifted ratio towards non-acidic autophagic vesicles when *Bchs* was overexpressed in glia suggest that the overexpression disrupts the autophagy pathway (Figures 3,4). Nevertheless, we cannot rule out that the formation of non-acidic autophagic vesicles was increased but the downstream autophagy pathway was limited by the fusion step, leading to an excessive build-up of non-acidic vesicles. Further, we cannot conclude on the nature of the accumulated cargo. For neuronal *Bchs* overexpression, the enriched GO terms related to mitochondria could imply that the degradation of those organelles was impaired, which would be in accordance with previous studies demonstrating that *WDFY3* haploinsufficiency in mice impairs mitophagy (Napoli *et al.*, 2018, 2021). However, this remains purely speculative and needs further investigation in future studies.

Additionally, neuronal and glial *Bchs* overexpression decreased mRNA levels of the autophagy-associated genes *Iml1* and *Rab32* (*lightoid*) (Table S1,2), further supporting a perturbed autophagic flux (Wang *et al.*, 2012; Wu & Tu, 2011). Interestingly, *rab32*, encoding a small GTPase, was previously proposed as a potential interaction partner of *Bchs* because a *rab32* mutation (*ltd-1*) enhanced the abnormal eye morphology induced by *Bchs* overexpression using *GMR-Gal4* (Simonsen *et al.*, 2007). The downregulation of *rab32* in glial and neuronal *Bchs* overexpression flies further implies that *Bchs* levels influence *rab32* transcription. *Iml1*,

encodes a protein that is involved in the negative regulation of the activity of mTORC1 (mechanistic target of rapamycin complex 1), an inhibitor of autophagy (Wei *et al.*, 2014). Noteworthy, levels of *mTor*, encoding the major component of mTORC1, are similarly decreased in neuronal *Bchs* overexpression flies, as well as several other modulators of mTORC1 signaling (*Nprl1*, *Nprl3*, *AMPKα*, *Nup44A*, *Rheb*, *RagA-B*, *PRAS40*) (Table S2). Thus, while Lu *et al.* suggested that mTORC1 inhibition increases expression of *Bchs* (Lu *et al.*, 2021), future studies should explore the effect of dysregulated *Bchs* levels on mTORC1 activity.

In both, larval and adult CNS, glial *Bchs* overexpression compared to neuronal *Bchs* overexpression resulted in a ref(2)P aggregation pattern that was more widely spread in the CNS (Figure 3). Noteworthy, fly heads of glial *Bchs* overexpression animals displayed a higher increase of the mRNA-fold change of *Bchs* than heads of neuronal *Bchs* overexpression flies (Figure 2(A)). Therefore, a stronger overexpression in the glial compared to the neuronal condition could contribute to the more prominent autophagic defect in glial *Bchs* overexpression flies. However, from ref(2)P accumulation it is not possible to conclude on the impact on neuronal function. Yet, recent research has shown that glial autophagy impacts neuronal health, for example., in neurodegenerative diseases like Parkinson's disease and Alzheimer's disease (Bankston *et al.*, 2019; Cho *et al.*, 2014; Choi *et al.*, 2020; Damulewicz *et al.*, 2022; Kreher *et al.*, 2021; Tu *et al.*, 2021; Szabó *et al.*, 2023). In conclusion, our data indicate that overexpression of *Bchs* can negatively impact autophagic flux.

4.3. Glial Bchs affects VNC morphology

In our study, only glial, but not neuronal, *Bchs* overexpression caused an elongated VNC (Figure 5). The elongation of the adult VNC might be an artefact caused by an abnormal tissue integrity like the observed fragility of the VNC in glial *Bchs* overexpression flies, which could lead to stretching of the VNC during dissection or mounting. Kadir *et al.* mentioned similar observations of atypical fragile and malformed brains of *Drosophila* pharates ubiquitously expressing mutant human *WDFY3* (Kadir *et al.,* 2016). Although, the expression of mutant *WDFY3* is scarcely comparable to our *Bchs* overexpression condition, it indicates that *WDFY3*/*Bchs* can affect the texture of CNS tissue. Nevertheless, an increase in cell number or cell size could also contribute to the VNC expansion. Importantly, glial *Bchs* overexpression resulted in a gain of glial nuclei number (Figure 5, S8D). This gain could have been caused by increased proliferation of *Drosophila* neural stem cells (neuroblasts), intermediate progenitor cells or glial cells. It is well known that glial cells can regulate neuroblast proliferation (Kanai *et al.*, 2018; Yang *et al.*, 2021; Nguyen & Cheng, 2022). For example, the expression of *Scarface*, a nutritionally sensitive gene, in subperineural glia modulates not only perineural glia proliferation but also neuroblast proliferation (Contreras *et al.*, 2021). However, reduced glial cell death could also have provoked a cell number increase. Furthermore, the glial subtype in which *Bchs* overexpression was sufficient to promote an elongated larval VNC, the subperineural glia, undergo nuclear divisions without a subsequent cytokinesis to turn into multinucleated cells, hereafter referred to as endomitosis (Unhavaithaya & Orr-Weaver, 2012; Orr-Weaver, 2015). Typically, only subperineural glia in brain lobes are multinucleated. However, it was demonstrated that endomitosis in subperineural glia of the VNC can be induced by reduced Notch signaling (Von Stetina *et al.*, 2018). Therefore, enhanced endomitosis of glia represents another possible mechanism for generating a gain in glial nuclei number. Further studies are needed, to determine whether the increased nuclei number is caused by alteration of proliferation, cell death or endomitosis. In addition, it would be interesting to design future experiments to test to which extent the glial nuclei number is impaired in adult flies, given the fact that in humans we observe an attenuation of the head circumference alteration with increasing age (Le Duc *et al.*, 2019).

Several genes have been previously associated with elongated VNC as seen in glial *Bchs* overexpression larvae (Figure 5(A)), for example, glial overexpression of the genes *mmp2* or *kuz,* encoding metalloproteases (Kato *et al.*, 2011; Pandey *et al.,* 2011; Meyer *et al.,* 2014; Losada-Perez *et al.*, 2016; Skeath *et al.*, 2017; Dai *et al.*, 2018; Luong *et al.*, 2018; Winkler *et al.*, 2021). Both proteases likely regulate BBB integrity (Kanda *et al.*, 2019; Petri *et al.*, 2019). Subperineural glia form an essential part of the BBB by producing septate junctions. Additionally, in our transcriptomic analyses we found a dysregulation of genes associated with septate junctions (*Tsf2*, *kune*, *cold*, *gli*, *hoka*, *udt*, Table S1) in flies overexpressing *Bchs* in glial cells (Schulte *et al.*, 2003; Nelson *et al.*, 2010; Tiklová *et al.*, 2010; Hijazi *et al.,* 2011; Kanda *et al.*, 2019; Izumi *et al.*, 2021). This suggests that glial *Bchs* overexpression impairs proper septate junction formation and BBB integrity, which could contribute to the increased VNC length.

Our data suggest that both, neuronal and glial *Bchs* upregulation contribute to neural defects. The overexpression approach employed in this study did not include a temporal control of the upregulation of *Bchs*. Hence, observed phenotypic impairments could have been provoked during any prior developmental stage. Future investigations could utilize *Gal80* fly strains for conditional *Bchs* overexpression to investigate more immediate effects of the overexpression on neural function (Mcguire *et al.,* 2003). Further studies should address whether *WDFY3* upregulation is similarly disadvantageous in other model organisms and human individuals. Moreover, glial dysregulation of *WDFY3*/*Bchs* should gain more attention when investigating *WDFY3*-associated pathologies.

Acknowledgements

We thank Anne Butthof for advices on RNA extraction protocol, Mathias Böhme for discussion about glial cells and Torsten Schöneberg for useful discussions which led to new insights in respect to the pathomechanism.

Author contributions

MK performed fly experiments, contributed to the experimental design and wrote the first draft of the manuscript. AV and LB performed gene expression and GO enrichment analyses. IS and JK performed PEDtracker assays and contributed to writing of the manuscript. KK, KD and JH performed RNA and DNA sequencing. AG, AT and RAJ contributed to result interpretation and writing of the manuscript. NS, AM and TL contributed to the design of the study, data interpretation, funding acquisition, and writing of the manuscript. DLD designed and supervised the study, acquired funding, and contributed to the writing of the manuscript.

Disclosure statement

No potential conflict of interest was reported by the author(s).

Availability of data and materials

RNA-seq data have been submitted to the Gene Expression Omnibus (https://www.ncbi.nlm.nih.gov/geo/query/acc.cgi?acc=GSE244775) under accession number GSE244775. The supplementary tables (Tables S1–S6) have been submitted to Zenodo (https://doi.org/10.5281/zenodo.14809796).

Funding

This work was supported by the Else Kröner-Fresenius-Stiftung 2020_EKEA.42 to DLD and the German Research Foundation SFB 1052 project B10 to DLD and AG. DLD and AM are fellows of the Clinician Scientist program of the Leipzig University Medical Center. AM received funding from Jung Foundation for Science and Research through Jung Career Advancement Prize 2023. NS and TL were funded by the German Research Foundation through CRC 1423, project B06 (project number 421152132). NS was supported through a Junior research grant from the Faculty of Medicine, Leipzig University. AT was supported by the German Research Foundation (Grant No. 441181781, 426722269, 432195391) and by EU funds from the ESF Plus Program (Grant No. 100649752). Mutant and transgenic fly stocks were obtained from the Bloomington Drosophila Stock Center (NIH P40OD018537).

ORCID

Marek B. Körner http://orcid.org/0000-0001-8221-8975
Andreas S. Thum http://orcid.org/0000-0002-3830-6596
Achmed Mrestani http://orcid.org/0000-0003-3063-164X
Nicole Scholz http://orcid.org/0000-0001-8087-8451
Tobias Langenhan http://orcid.org/0000-0002-9061-3809
Diana Le Duc http://orcid.org/0000-0001-7289-2552

References

Aber, E. R., Griffey, C. J., Davies, T., Li, A. M., Yang, Y. J., Croce, K. R., Goldman, J. E., Grutzendler, J., Canman, J. C., & Yamamoto, A. (2022). Oligodendroglial macroautophagy is essential for myelin sheath turnover to prevent neurodegeneration and death. *Cell Reports*, *41*(3), 111480. https://doi.org/10.1016/j.celrep.2022.111480

Anders, S., Pyl, P. T., & Huber, W. (2015). HTSeq—a Python framework to work with high-throughput sequencing data. *Bioinformatics (Oxford, England)*, *31*(2), 166–169. https://doi.org/10.1093/bioinformatics/btu638

Arai, T., Hasegawa, M., Akiyama, H., Ikeda, K., Nonaka, T., Mori, H., Mann, D., Tsuchiya, K., Yoshida, M., Hashizume, Y., & Oda, T. (2006). TDP-43 is a component of ubiquitin-positive tau-negative inclusions in frontotemporal lobar degeneration and amyotrophic lateral sclerosis. *Biochemical and Biophysical Research Communications*, *351*(3), 602–611. https://doi.org/10.1016/j.bbrc.2006.10.093

Bankston, A. N., Forston, M. D., Howard, R. M., Andres, K. R., Smith, A. E., Ohri, S. S., Bates, M. L., Bunge, M. B., & Whittemore, S. R. (2019). Autophagy is essential for oligodendrocyte differentiation, survival, and proper myelination. *Glia*, *67*(9), 1745–1759. https://doi.org/10.1002/glia.23646

Bartlett, B. J., Isakson, P., Lewerenz, J., Sanchez, H., Kotzebue, R. W., Cumming, R. C., Harris, G. L., Nezis, I. P., Schubert, D. R., Simonsen, A., & Finley, K. D. (2011). p62, Ref(2)P and ubiquitinated proteins are conserved markers of neuronal aging, aggregate formation and progressive autophagic defects. *Autophagy*, *7*(6), 572–583. https://doi.org/10.4161/auto.7.6.14943

Baumgartner, S., Littleton, J. T., Broadie, K., Bhat, M. A., Harbecke, R., Lengyel, J. A., Chiquet-Ehrismann, R., Prokop, A., & Bellen, H. J. (1996). A Drosophila neurexin is required for septate junction and blood-nerve barrier formation and function. *Cell*, *87*(6), 1059–1068. https://doi.org/10.1016/s0092-8674(00)81800-0

Benjamini, Y., Drai, D., Elmer, G., Kafkafi, N., & Golani, I. (2001). Controlling the false discovery rate in behavior genetics research. *Behavioural Brain Research*, *125*(1-2), 279–284. https://doi.org/10.1016/s0166-4328(01)00297-2

Berni, J., Pulver, S. R., Griffith, L. C., & Bate, M. (2012). Autonomous circuitry for substrate exploration in freely moving Drosophila larvae. *Current Biology: CB*, *22*(20), 1861–1870. https://doi.org/10.1016/j.cub.2012.07.048

Bittern, J., Pogodalla, N., Ohm, H., Brüser, L., Kottmeier, R., Schirmeier, S., & Klämbt, C. (2021). Neuron-glia interaction in the Drosophila nervous system. *Developmental Neurobiology*, *81*(5), 438–452. https://doi.org/10.1002/dneu.22737

Carlson, M. (2019). *org.Dm.eg.db: Genome wide annotation for Fly. R package version 3.8.2.*

Cho, M.-H., Cho, K., Kang, H.-J., Jeon, E.-Y., Kim, H.-S., Kwon, H.-J., Kim, H.-M., Kim, D.-H., & Yoon, S.-Y. (2014). Autophagy in microglia degrades extracellular β-amyloid fibrils and regulates the NLRP3 inflammasome. *Autophagy*, *10*(10), 1761–1775. https://doi.org/10.4161/auto.29647

Choi, I., Zhang, Y., Seegobin, S. P., Pruvost, M., Wang, Q., Purtell, K., Zhang, B., & Yue, Z. (2020). Microglia clear neuron-released α-synuclein via selective autophagy and prevent neurodegeneration. *Nature Communications*, *11*(1), 1386. https://doi.org/10.1038/s41467-020-15119-w

Clausen, T. H., Lamark, T., Isakson, P., Finley, K., Larsen, K. B., Brech, A., Øvervatn, A., Stenmark, H., Bjørkøy, G., Simonsen, A., & Johansen, T. (2010). p62/SQSTM1 and ALFY interact to facilitate the formation of p62 bodies/ALIS and their degradation by autophagy. *Autophagy*, *6*(3), 330–344. https://doi.org/10.4161/auto.6.3.11226

Contreras, E. G., Glavic, Á., Brand, A. H., & Sierralta, J. A. (2021). The serine protease homolog, scarface, is sensitive to nutrient availability and modulates the development of the drosophila blood-brain barrier. *The Journal of Neuroscience: The Official Journal of the Society for Neuroscience*, *41*(30), 6430–6448. https://doi.org/10.1523/JNEUROSCI.0452-20.2021

Dai, J., Estrada, B., Jacobs, S., Sánchez-Sánchez, B. J., Tang, J., Ma, M., Magadán-Corpas, P., Pastor-Pareja, J. C., & Martín-Bermudo, M. D. (2018). Dissection of Nidogen function in Drosophila reveals tissue-specific mechanisms of basement membrane assembly. *PLoS Genetics*, *14*(9), e1007483. https://doi.org/10.1371/journal.pgen.1007483

Damulewicz, M., Szypulski, K., & Pyza, E. (2022). Glia-neurons cross-talk regulated through autophagy. *Frontiers in Physiology*, *13*, 886273. https://doi.org/10.3389/fphys.2022.886273

Dewey, E. M., McNabb, S. L., Ewer, J., Kuo, G. R., Takanishi, C. L., Truman, J. W., & Honegger, H.-W. (2004). Identification of the gene encoding bursicon, an insect neuropeptide responsible for cuticle sclerotization and wing spreading. *Current Biology: CB*, *14*(13), 1208–1213. https://doi.org/10.1016/j.cub.2004.06.051

DiAntonio, A., Burgess, R. W., Chin, A. C., Deitcher, D. L., Scheller, R. H., & Schwarz, T. L. (1993). Identification and characterization of Drosophila genes for synaptic vesicle proteins. *The Journal of Neuroscience: The Official Journal of the Society for Neuroscience*, *13*(11), 4924–4935. https://doi.org/10.1523/JNEUROSCI.13-11-04924.1993

Dobin, A., Davis, C. A., Schlesinger, F., Drenkow, J., Zaleski, C., Jha, S., Batut, P., Chaisson, M., & Gingeras, T. R. (2013). STAR: ultrafast universal RNA-seq aligner. *Bioinformatics (Oxford, England)*, *29*(1), 15–21. https://doi.org/10.1093/bioinformatics/bts635

Dragich, J. M., Kuwajima, T., Hirose-Ikeda, M., Yoon, M. S., Eenjes, E., Bosco, J. R., Fox, L. M., Lystad, A. H., Oo, T. F., Yarygina, O., Mita, T., Waguri, S., Ichimura, Y., Komatsu, M., Simonsen, A., Burke, R. E., Mason, C. A., & Yamamoto, A. (2016). Autophagy linked FYVE (Alfy/WDFY3) is required for establishing neuronal connectivity in the mammalian brain. *eLife*, *5*, e14810. https://doi.org/10.7554/eLife.14810

Filimonenko, M., Isakson, P., Finley, K. D., Anderson, M., Jeong, H., Melia, T. J., Bartlett, B. J., Myers, K. M., Birkeland, H. C. G., Lamark, T., Krainc, D., Brech, A., Stenmark, H., Simonsen, A., & Yamamoto, A. (2010). The selective macroautophagic degradation of aggregated proteins requires the PI3P-binding protein Alfy. *Molecular Cell*, *38*(2), 265–279. https://doi.org/10.1016/j.molcel.2010.04.007

Finley, K. D., Edeen, P. T., Cumming, R. C., Mardahl-Dumesnil, M. D., Taylor, B. J., Rodriguez, M. H., Hwang, C. E., Benedetti, M., & McKeown, M. (2003). Blue cheese mutations define a novel, conserved gene involved in progressive neural degeneration. *The Journal of Neuroscience: The Official Journal of the Society for Neuroscience*, *23*(4), 1254–1264. https://doi.org/10.1523/JNEUROSCI.23-04-01254.2003

Firth, H. V., Richards, S. M., Bevan, A. P., Clayton, S., Corpas, M., Rajan, D., Van Vooren, S., Moreau, Y., Pettett, R. M., & Carter, N. P. (2009). DECIPHER: Database of chromosomal imbalance and phenotype in humans using Ensembl resources. *American Journal of Human Genetics*, *84*(4), 524–533. https://doi.org/10.1016/j.ajhg.2009.03.010

Fox, L. M., Kim, K., Johnson, C. W., Chen, S., Croce, K. R., Victor, M. B., Eenjes, E., Bosco, J. R., Randolph, L. K., Dragatsis, I., Dragich, J. M., Yoo, A. S., & Yamamoto, A. (2020). Huntington's disease pathogenesis is modified in vivo by Alfy/Wdfy3 and selective macroautophagy. *Neuron*, *105*(5), 813–821.e6. https://doi.org/10.1016/j.neuron.2019.12.003

Gao, Y. L., Wang, N., Sun, F. R., Cao, X. P., Zhang, W., & Yu, J. T. (2018). Tau in neurodegenerative disease. *Annals of Translational Medicine*, *6*(10), 175–175. https://doi.org/10.21037/atm.2018.04.23

Goedert, M., Crowther, R. A., Scheres, S. H. W., & Spillantini, M. G. (2024). Tau and neurodegeneration. *Cytoskeleton (Hoboken, N.J.)*, *81*(1), 95–102. https://doi.org/10.1002/cm.21812

Gowda, S. B. M., Salim, S., & Mohammad, F. (2021). Anatomy and neural pathways modulating distinct locomotor behaviors in drosophila larva. *Biology*, *10*(2), 90. https://doi.org/10.3390/biology10020090

Han, H., Wei, W., Duan, W., Guo, Y., Li, Y., Wang, J., Bi, Y., & Li, C. (2015). Autophagy-linked FYVE protein (Alfy) promotes autophagic removal of misfolded proteins involved in amyotrophic lateral sclerosis (ALS). *In Vitro Cellular & Developmental Biology. Animal*, *51*(3), 249–263. https://doi.org/10.1007/s11626-014-9832-4

Hebbar, S., Sahoo, I., Matysik, A., Argudo Garcia, I., Osborne, K. A., Papan, C., Torta, F., Narayanaswamy, P., Fun, X. H., Wenk, M. R., Shevchenko, A., Schwudke, D., & Kraut, R. (2015). Ceramides and stress signalling intersect with autophagic defects in neurodegenerative Drosophila blue cheese (bchs) mutants. *Scientific Reports*, *5*(1), 15926. https://doi.org/10.1038/srep15926

Hijazi, A., Haenlin, M., Waltzer, L., & Roch, F. (2011). The Ly6 protein coiled is required for septate junction and blood brain barrier organisation in Drosophila. *PLoS One*, *6*(3), e17763. https://doi.org/10.1371/journal.pone.0017763

Hirota, Y., & Tanaka, Y. (2009). A small GTPase, human Rab32, is required for the formation of autophagic vacuoles under basal conditions. *Cellular and Molecular Life Sciences: CMLS*, *66*(17), 2913–2932. https://doi.org/10.1007/s00018-009-0080-9

Izumi, Y., Furuse, K., & Furuse, M. (2021). The novel membrane protein Hoka regulates septate junction organization and stem cell homeostasis in the Drosophila gut. *Journal of Cell Science*, *134*(6), jcs257022. https://doi.org/10.1242/jcs.257022

Jain, A., Rusten, T. E., Katheder, N., Elvenes, J., Bruun, J.-A., Sjøttem, E., Lamark, T., & Johansen, T. (2015). p62/Sequestosome-1, autophagy-related gene 8, and autophagy in drosophila are regulated by nuclear factor erythroid 2-related factor 2 (NRF2), independent of transcription factor TFEB. *The Journal of Biological Chemistry*, *290*(24), 14945–14962. https://doi.org/10.1074/jbc.M115.656116

Kabashi, E., Valdmanis, P. N., Dion, P., Spiegelman, D., McConkey, B. J., Vande Velde, C., Bouchard, J.-P., Lacomblez, L., Pochigaeva, K., Salachas, F., Pradat, P.-F., Camu, W., Meininger, V., Dupre, N., & Rouleau, G. A. (2008). TARDBP mutations in individuals with sporadic and familial amyotrophic lateral sclerosis. *Nature Genetics*, *40*(5), 572–574. https://doi.org/10.1038/ng.132

Kadir, R., Harel, T., Markus, B., Perez, Y., Bakhrat, A., Cohen, I., Volodarsky, M., Feintsein-Linial, M., Chervinski, E., Zlotogora, J., Sivan, S., Birnbaum, R. Y., Abdu, U., Shalev, S., & Birk, O. S. (2016). ALFY-controlled DVL3 autophagy regulates Wnt signaling, determining human brain size. *PLoS Genetics*, *12*(3), e1005919. https://doi.org/10.1371/journal.pgen.1005919

Kanai, M. I., Kim, M. J., Akiyama, T., Takemura, M., Wharton, K., O'Connor, M. B., & Nakato, H. (2018). Regulation of neuroblast proliferation by surface glia in the Drosophila larval brain. *Scientific Reports*, *8*(1), 3730. https://doi.org/10.1038/s41598-018-22028-y

Kanda, H., Shimamura, R., Koizumi-Kitajima, M., & Okano, H. (2019). Degradation of extracellular matrix by matrix metalloproteinase 2 is essential for the establishment of the blood-brain barrier in drosophila. *iScience*, *16*, 218–229. https://doi.org/10.1016/j.isci.2019.05.027

Karlsson, M., Zhang, C., Méar, L., Zhong, W., Digre, A., Katona, B., Sjöstedt, E., Butler, L., Odeberg, J., Dusart, P., Edfors, F., Oksvold, P., von Feilitzen, K., Zwahlen, M., Arif, M., Altay, O., Li, X., Ozcan, M., Mardinoglu, A., … Lindskog, C. (2021). A single-cell type transcriptomics map of human tissues. *Science Advances*, *7*(31), eabh2169. https://doi.org/10.1126/sciadv.abh2169

Kato, K., Forero, M. G., Fenton, J. C., & Hidalgo, A. (2011). The glial regenerative response to central nervous system injury is enabled by pros-notch and pros-NFκB feedback. *PLoS Biology*, *9*(8), e1001133. https://doi.org/10.1371/journal.pbio.1001133

Khodosh, R., Augsburger, A., Schwarz, T. L., & Garrity, P. A. (2006). Bchs, a BEACH domain protein, antagonizes Rab11 in synapse morphogenesis and other developmental events. *Development (Cambridge, England)*, *133*(23), 4655–4665. https://doi.org/10.1242/dev.02650

Kim, Y. S., Choi, J., & Yoon, B.-E. (2020). Neuron-glia interactions in neurodevelopmental disorders. *Cells*, *9*(10), 2176. https://doi.org/10.3390/cells9102176

Körner, M. B., Velluva, A., Bundalian, L., Radtke, M., Lin, C.-C., Zacher, P., Bartolomaeus, T., Kirstein, A. S., Mrestani, A., Scholz, N., Platzer, K., Teichmann, A.-C., Hentschel, J., Langenhan, T., Lemke, J. R., Garten, A., Abou Jamra, R., & Le Duc, D. (2022). Altered gene expression profiles impair the nervous system development in individuals with 15q13.3 microdeletion. *Scientific Reports*, *12*(1), 13507. https://doi.org/10.1038/s41598-022-17604-2

Kraut, R., Menon, K., & Zinn, K. (2001). A gain-of-function screen for genes controlling motor axon guidance and synaptogenesis in Drosophila. *Current Biology: CB*, *11*(6), 417–430. https://doi.org/10.1016/S0960-9822(01)00124-5

Kreher, C., Favret, J., Maulik, M., & Shin, D. (2021). Lysosomal functions in glia associated with neurodegeneration. *Biomolecules*, *11*(3), 400. https://doi.org/10.3390/biom11030400

Kriston-Vizi, J., Thong, N. W., Poh, C. L., Yee, K. C., Ling, J. S. P., Kraut, R., & Wasser, M. (2011). Gebiss: an ImageJ plugin for the specification of ground truth and the performance evaluation of 3D

segmentation algorithms. *BMC Bioinformatics*, *12*(1), 232. https://doi.org/10.1186/1471-2105-12-232

Lago-Baldaia, I., Fernandes, V. M., & Ackerman, S. D. (2020). More than mortar: glia as architects of nervous system development and disease. *Frontiers in Cell and Developmental Biology*, *8*, 611269. https://doi.org/10.3389/fcell.2020.611269

Lahr, E. C., Dean, D., & Ewer, J. (2012). Genetic analysis of ecdysis behavior in Drosophila reveals partially overlapping functions of two unrelated neuropeptides. *The Journal of Neuroscience: The Official Journal of the Society for Neuroscience*, *32*(20), 6819–6829. https://doi.org/10.1523/JNEUROSCI.5301-11.2012

Laneve, P., Piacentini, L., Casale, A. M., Capauto, D., Gioia, U., Cappucci, U., Di Carlo, V., Bozzoni, I., Di Micco, P., Morea, V., Di Franco, C. A., & Caffarelli, E. (2017). Drosophila CG3303 is an essential endoribonuclease linked to TDP-43-mediated neurodegeneration. *Scientific Reports*, *7*(1), 41559. https://doi.org/10.1038/srep41559

Le Duc, D., Giulivi, C., Hiatt, S. M., Napoli, E., Panoutsopoulos, A., Harlan De Crescenzo, A., Kotzaeridou, U., Syrbe, S., Anagnostou, E., Azage, M., Bend, R., Begtrup, A., Brown, N. J., Büttner, B., Cho, M. T., Cooper, G. M., Doering, J. H., Dubourg, C., Everman, D. B., … Jamra, R. (2019). Pathogenic WDFY3 variants cause neurodevelopmental disorders and opposing effects on brain size. *Brain: A Journal of Neurology*, *142*(9), 2617–2630. https://doi.org/10.1093/brain/awz198

Lim, A., & Kraut, R. (2009). The Drosophila BEACH family protein, blue cheese, links lysosomal axon transport with motor neuron degeneration. *The Journal of Neuroscience: The Official Journal of the Society for Neuroscience*, *29*(4), 951–963. https://doi.org/10.1523/JNEUROSCI.2582-08.2009

Losada-Perez, M., Harrison, N., & Hidalgo, A. (2016). Molecular mechanism of central nervous system repair by the Drosophila NG2 homologue kon-tiki. *The Journal of Cell Biology*, *214*(5), 587–601. https://doi.org/10.1083/jcb.201603054

Love, M. I., Huber, W., & Anders, S. (2014). Moderated estimation of fold change and dispersion for RNA-seq data with DESeq2. *Genome Biology*, *15*(12), 550. https://doi.org/10.1186/s13059-014-0550-8

Loveall, B. J., & Deitcher, D. L. (2010). The essential role of bursicon during Drosophila development. *BMC Developmental Biology*, *10*(1), 92. https://doi.org/10.1186/1471-213X-10-92

Luan, H., Lemon, W. C., Peabody, N. C., Pohl, J. B., Zelensky, P. K., Wang, D., Nitabach, M. N., Holmes, T. C., & White, B. H. (2006). Functional dissection of a neuronal network required for cuticle tanning and wing expansion in Drosophila. *The Journal of Neuroscience: The Official Journal of the Society for Neuroscience*, *26*(2), 573–584. https://doi.org/10.1523/JNEUROSCI.3916-05.2006

Lu, Y.-X., Regan, J. C., Eßer, J., Drews, L. F., Weinseis, T., Stinn, J., Hahn, O., Miller, R. A., Grönke, S., & Partridge, L. (2021). A TORC1-histone axis regulates chromatin organisation and non-canonical induction of autophagy to ameliorate ageing. *eLife*, *10*, e62233. https://doi.org/10.7554/eLife.62233

Luo, C. W., Dewey, E. M., Sudo, S., Ewer, J., Hsu, S. Y., Honegger, H.-W., & Hsueh, A. J. W. (2005). Bursicon, the insect cuticle-hardening hormone, is a heterodimeric cystine knot protein that activates G protein-coupled receptor LGR2. *Proceedings of the National Academy of Sciences of the United States of America*, *102*(8), 2820–2825. https://doi.org/10.1073/pnas.0409916102

Luong, D., Perez, L., & Jemc, J. C. (2018). Identification of raw as a regulator of glial development. *PLoS ONE*, *13*(5), e0198161. https://doi.org/10.1371/journal.pone.0198161

Marini, F., & Binder, H. (2019). pcaExplorer: an R/Bioconductor package for interacting with RNA-seq principal components. *BMC Bioinformatics*, *20*(1), 331. https://doi.org/10.1186/s12859-019-2879-1

Marqués, G., Bao, H., Haerry, T. E., Shimell, M. J., Duchek, P., Zhang, B., & O'Connor, M. B. (2002). The Drosophila BMP type II receptor Wishful Thinking regulates neuromuscular synapse morphology and function. *Neuron*, *33*(4), 529–543. https://doi.org/10.1016/s0896-6273(02)00595-0

McGuire, S. E., Le, P. T., Osborn, A. J., Matsumoto, K., & Davis, R. L. (2003). Spatiotemporal rescue of memory dysfunction in Drosophila. *Science (New York, N.Y.)*, *302*(5651), 1765–1768. https://doi.org/10.1126/science.1089035

Mercer, S. W., La Fontaine, S., Warr, C. G., & Burke, R. (2016). Reduced glutathione biosynthesis in Drosophila melanogaster causes neuronal defects linked to copper deficiency. *Journal of Neurochemistry*, *137*(3), 360–370. https://doi.org/10.1111/jnc.13567

Meyer, S., Schmidt, I., & Klämbt, C. (2014). Glia ECM interactions are required to shape the Drosophila nervous system. *Mechanisms of Development*, *133*, 105–116. https://doi.org/10.1016/j.mod.2014.05.003

Napoli, E., Panoutsopoulos, A. A., Kysar, P., Satriya, N., Sterling, K., Shibata, B., Imai, D., Ruskin, D. N., Zarbalis, K. S., & Giulivi, C. (2021). Wdfy3 regulates glycophagy, mitophagy, and synaptic plasticity. *Journal of Cerebral Blood Flow and Metabolism: Official Journal of the International Society of Cerebral Blood Flow and Metabolism*, *41*(12), 3213–3231. 271678X211027384. https://doi.org/10.1177/0271678X211027384

Napoli, E., Song, G., Panoutsopoulos, A., Riyadh, M. A., Kaushik, G., Halmai, J., Levenson, R., Zarbalis, K. S., & Giulivi, C. (2018). Beyond autophagy: a novel role for autism-linked Wdfy3 in brain mitophagy. *Scientific Reports*, *8*(1), 11348. https://doi.org/10.1038/s41598-018-29421-7

Nelson, K. S., Furuse, M., & Beitel, G. J. (2010). The Drosophila Claudin Kune-kune is required for septate junction organization and tracheal tube size control. *Genetics*, *185*(3), 831–839. https://doi.org/10.1534/genetics.110.114959

Neumann, M., Sampathu, D. M., Kwong, L. K., Truax, A. C., Micsenyi, M. C., Chou, T. T., Bruce, J., Schuck, T., Grossman, M., Clark, C. M., McCluskey, L. F., Miller, B. L., Masliah, E., Mackenzie, I. R., Feldman, H., Feiden, W., Kretzschmar, H. A., Trojanowski, J. Q., & Lee, V. M.-Y. (2006). Ubiquitinated TDP-43 in frontotemporal lobar degeneration and amyotrophic lateral sclerosis. *Science (New York, N.Y.)*, *314*(5796), 130–133. https://doi.org/10.1126/science.1134108

Nezis, I. P., Shravage, B. V., Sagona, A. P., Lamark, T., Bjørkøy, G., Johansen, T., Rusten, T. E., Brech, A., Baehrecke, E. H., & Stenmark, H. (2010). Autophagic degradation of dBruce controls DNA fragmentation in nurse cells during late Drosophila melanogaster oogenesis. *The Journal of Cell Biology*, *190*(4), 523–531. https://doi.org/10.1083/jcb.201002035

Nezis, I. P., Simonsen, A., Sagona, A. P., Finley, K., Gaumer, S., Contamine, D., Rusten, T. E., Stenmark, H., & Brech, A. (2008). Ref(2)P, the Drosophila melanogaster homologue of mammalian p62, is required for the formation of protein aggregates in adult brain. *The Journal of Cell Biology*, *180*(6), 1065–1071. https://doi.org/10.1083/jcb.200711108

Nguyen, P.-K., & Cheng, L. Y. (2022). Non-autonomous regulation of neurogenesis by extrinsic cues: a Drosophila perspective. *Oxford Open Neuroscience*, *1*, kvac004. https://doi.org/10.1093/oons/kvac004

Orosco, L. A., Ross, A. P., Cates, S. L., Scott, S. E., Wu, D., Sohn, J., Pleasure, D., Pleasure, S. J., Adamopoulos, I. E., & Zarbalis, K. S. (2014). Loss of Wdfy3 in mice alters cerebral cortical neurogenesis reflecting aspects of the autism pathology. *Nature Communications*, *5*(1), 4692. https://doi.org/10.1038/ncomms5692

Orr-Weaver, T. L. (2015). When bigger is better: The role of polyploidy in organogenesis. *Trends in Genetics: TIG*, *31*(6), 307–315. https://doi.org/10.1016/j.tig.2015.03.011

Pandey, R., Blanco, J., & Udolph, G. (2011). The glucuronyltransferase GlcAT-P is required for stretch growth of peripheral nerves in Drosophila. *PLoS One*, *6*(11), e28106. https://doi.org/10.1371/journal.pone.0028106

Park, J. H., Schroeder, A. J., Helfrich-Förster, C., Jackson, F. R., & Ewer, J. (2003). Targeted ablation of CCAP neuropeptide-containing neurons of Drosophila causes specific defects in execution and circadian timing of ecdysis behavior. *Development (Cambridge, England)*, *130*(12), 2645–2656. https://doi.org/10.1242/dev.00503

Peabody, N. C., Diao, F., Luan, H., Wang, H., Dewey, E. M., Honegger, H.-W., & White, B. H. (2008). Bursicon functions within the Drosophila CNS to modulate wing expansion behavior, hormone secretion, and cell death. *The Journal of Neuroscience: The Official Journal of the Society for Neuroscience*, *28*(53), 14379–14391. https://doi.org/10.1523/JNEUROSCI.2842-08.2008

Peabody, N. C., Pohl, J. B., Diao, F., Vreede, A. P., Sandstrom, D. J., Wang, H., Zelensky, P. K., & White, B. H. (2009). Characterization

of the decision network for wing expansion in Drosophila using targeted expression of the TRPM8 channel. *The Journal of Neuroscience: The Official Journal of the Society for Neuroscience*, *29*(11), 3343–3353. https://doi.org/10.1523/JNEUROSCI.4241-08.2009

Petri, J., Syed, M. H., Rey, S., & Klämbt, C. (2019). Non-cell-autonomous function of the GPI-anchored protein Undicht during septate junction assembly. *Cell Reports*, *26*(6), 1641–1653.e4. https://doi.org/10.1016/j.celrep.2019.01.046

Pircs, K., Nagy, P., Varga, A., Venkei, Z., Erdi, B., Hegedus, K., & Juhasz, G. (2012). Advantages and limitations of different p62-based assays for estimating autophagic activity in Drosophila. *PLoS ONE*, *7*(8), e44214. https://doi.org/10.1371/journal.pone.0044214

Pulver, S. R., Bayley, T. G., Taylor, A. L., Berni, J., Bate, M., & Hedwig, B. (2015). Imaging fictive locomotor patterns in larval Drosophila. *Journal of Neurophysiology*, *114*(5), 2564–2577. https://doi.org/10.1152/jn.00731.2015

Rahman, M. M., Islam, M. R., Yamin, M., Islam, M. M., Sarker, M. T., Meem, A. F. K., Akter, A., Emran, T. B., Cavalu, S., & Sharma, R. (2022). Emerging role of neuron-glia in neurological disorders: At a glance. *Oxidative Medicine and Cellular Longevity*, *2022*, 3201644–27. https://doi.org/10.1155/2022/3201644

Schaaf, Z. A., Tat, L., Cannizzaro, N., Panoutsopoulos, A. A., Green, R., Rülicke, T., Hippenmeyer, S., & Zarbalis, K. S. (2022). WDFY3 mutation alters laminar position and morphology of cortical neurons. *Molecular Autism*, *13*(1), 27. https://doi.org/10.1186/s13229-022-00508-3

Schneider, C. A., Rasband, W. S., & Eliceiri, K. W. (2012). NIH Image to ImageJ: 25 years of image analysis. *Nature Methods*, *9*(7), 671–675. https://doi.org/10.1038/nmeth.2089

Schulte, J., Tepass, U., & Auld, V. J. (2003). Gliotactin, a novel marker of tricellular junctions, is necessary for septate junction development in Drosophila. *The Journal of Cell Biology*, *161*(5), 991–1000. https://doi.org/10.1083/jcb.200303192

Schumann, I., & Triphan, T. (2020). The PEDtracker: An automatic staging approach for Drosophila melanogaster larvae. *Frontiers in Behavioral Neuroscience*, *14*, 612313. https://doi.org/10.3389/fnbeh.2020.612313

Sepp, K. J., & Auld, V. J. (1999). Conversion of lacZ enhancer trap lines to GAL4 lines using targeted transposition in Drosophila melanogaster. *Genetics*, *151*(3), 1093–1101. https://doi.org/10.1093/genetics/151.3.1093

Sepp, K. J., Schulte, J., & Auld, V. J. (2001). Peripheral glia direct axon guidance across the CNS/PNS transition zone. *Developmental Biology*, *238*(1), 47–63. https://doi.org/10.1006/dbio.2001.0411

Sim, J., Osborne, K. A., Argudo García, I., Matysik, A. S., & Kraut, R. (2019). The BEACH domain is critical for blue cheese function in a spatial and epistatic autophagy hierarchy. *Frontiers in Cell and Developmental Biology*, *7*, 129. https://doi.org/10.3389/fcell.2019.00129

Simonsen, A., Birkeland, H. C. G., Gillooly, D. J., Mizushima, N., Kuma, A., Yoshimori, T., Slagsvold, T., Brech, A., & Stenmark, H. (2004). Alfy, a novel FYVE-domain-containing protein associated with protein granules and autophagic membranes. *Journal of Cell Science*, *117*(Pt 18), 4239–4251. https://doi.org/10.1242/jcs.01287

Simonsen, A., Cumming, R. C., Lindmo, K., Galaviz, V., Cheng, S., Rusten, T. E., & Finley, K. D. (2007). Genetic modifiers of the Drosophila blue cheese gene link defects in lysosomal transport with decreased life span and altered ubiquitinated-protein profiles. *Genetics*, *176*(2), 1283–1297. https://doi.org/10.1534/genetics.106.065011

Skeath, J. B., Wilson, B. A., Romero, S. E., Snee, M. J., Zhu, Y., & Lacin, H. (2017). The extracellular metalloprotease AdamTS-A anchors neural lineages in place within and preserves the architecture of the central nervous system. *Development (Cambridge, England)*, *144*(17), 3102–3113. https://doi.org/10.1242/dev.145854

Søreng, K., Pankiv, S., Bergsmark, C., Haugsten, E. M., Dahl, A. K., de la Ballina, L. R., Yamamoto, A., Lystad, A. H., & Simonsen, A. (2022). ALFY localizes to early endosomes and cellular protrusions to facilitate directional cell migration. *Journal of Cell Science*, *135*(4), jcs259138. https://doi.org/10.1242/jcs.259138

Stessman, H. A. F., Xiong, B., Coe, B. P., Wang, T., Hoekzema, K., Fenckova, M., Kvarnung, M., Gerdts, J., Trinh, S., Cosemans, N., Vives, L., Lin, J., Turner, T. N., Santen, G., Ruivenkamp, C., Kriek, M., van Haeringen, A., Aten, E., Friend, K., … Eichler, E. E. (2017). Targeted sequencing identifies 91 neurodevelopmental-disorder risk genes with autism and developmental-disability biases. *Nature Genetics*, *49*(4), 515–526. https://doi.org/10.1038/ng.3792

Stewart, B. A., Atwood, H. L., Renger, J. J., Wang, J., & Wu, C. F. (1994). Improved stability of Drosophila larval neuromuscular preparations in haemolymph-like physiological solutions. *Journal of Comparative Physiology. A, Sensory, Neural, and Behavioral Physiology*, *175*(2), 179–191. https://doi.org/10.1007/BF00215114

Stork, T., Engelen, D., Krudewig, A., Silies, M., Bainton, R. J., & Klämbt, C. (2008). Organization and function of the blood-brain barrier in Drosophila. *The Journal of Neuroscience: The Official Journal of the Society for Neuroscience*, *28*(3), 587–597. https://doi.org/10.1523/JNEUROSCI.4367-07.2008

Szabó, Á., Vincze, V., Chhatre, A. S., Jipa, A., Bognár, S., Varga, K. E., Banik, P., Harmatos-Ürmösi, A., Neukomm, L. J., & Juhász, G. (2023). LC3-associated phagocytosis promotes glial degradation of axon debris after injury in Drosophila models. *Nature Communications*, *14*(1), 3077. https://doi.org/10.1038/s41467-023-38755-4

Tiklová, K., Senti, K.-A., Wang, S., Gräslund, A., & Samakovlis, C. (2010). Epithelial septate junction assembly relies on melanotransferrin iron binding and endocytosis in Drosophila. *Nature Cell Biology*, *12*(11), 1071–1077. https://doi.org/10.1038/ncb2111

Tu, H.-Y., Yuan, B.-S., Hou, X.-O., Zhang, X.-J., Pei, C.-S., Ma, Y.-T., Yang, Y.-P., Fan, Y., Qin, Z.-H., Liu, C.-F., & Hu, L.-F. (2021). α-synuclein suppresses microglial autophagy and promotes neurodegeneration in a mouse model of Parkinson's disease. *Aging Cell*, *20*(12), e13522. https://doi.org/10.1111/acel.13522

Unhavaithaya, Y., & Orr-Weaver, T. L. (2012). Polyploidization of glia in neural development links tissue growth to blood-brain barrier integrity. *Genes and Development*, *26*(1), 31–36. https://doi.org/10.1101/gad.177436.111

Vanden Broeck, L., Naval-Sánchez, M., Adachi, Y., Diaper, D., Dourlen, P., Chapuis, J., Kleinberger, G., Gistelinck, M., Van Broeckhoven, C., Lambert, J. C., Hirth, F., Aerts, S., Callaerts, P., & Dermaut, B. (2013). TDP-43 loss-of-function causes neuronal loss due to defective steroid receptor-mediated gene program switching in Drosophila. *Cell Reports*, *3*(1), 160–172. https://doi.org/10.1016/j.celrep.2012.12.014

Von Stetina, J. R., Frawley, L. E., Unhavaithaya, Y., & Orr-Weaver, T. L. (2018). Variant cell cycles regulated by Notch signaling control cell size and ensure a functional blood-brain barrier. *Development (Cambridge, England)*, *145*(3), dev157115. https://doi.org/10.1242/dev.157115

Wang, T., Guo, H., Xiong, B., Stessman, H. A. F., Wu, H., Coe, B. P., Turner, T. N., Liu, Y., Zhao, W., Hoekzema, K., Vives, L., Xia, L., Tang, M., Ou, J., Chen, B., Shen, Y., Xun, G., Long, M., Lin, J., … Eichler, E. E. (2016). De novo genic mutations among a Chinese autism spectrum disorder cohort. *Nature Communications*, *7*(1), 13316. https://doi.org/10.1038/ncomms13316

Wang, C., Liu, Z., & Huang, X. (2012). Rab32 is important for autophagy and lipid storage in Drosophila. *PLoS ONE*, *7*(2), e32086. https://doi.org/10.1371/journal.pone.0032086

Wei, Y., Reveal, B., Reich, J., Laursen, W. J., Senger, S., Akbar, T., Iida-Jones, T., Cai, W., Jarnik, M., & Lilly, M. A. (2014). TORC1 regulators Iml1/GATOR1 and GATOR2 control meiotic entry and oocyte development in Drosophila. *Proceedings of the National Academy of Sciences of the United States of America*, *111*(52), E5670–7. https://doi.org/10.1073/pnas.1419156112

Winkler, B., Funke, D., Benmimoun, B., Spéder, P., Rey, S., Logan, M. A., & Klämbt, C. (2021). Brain inflammation triggers macrophage invasion across the blood-brain barrier in Drosophila during pupal stages. *Science Advances*, *7*(44), eabh0050. https://doi.org/10.1126/sciadv.abh0050

Wu, T., Hu, E., Xu, S., Chen, M., Guo, P., Dai, Z., Feng, T., Zhou, L., Tang, W., Zhan, L., Fu, X., Liu, S., Bo, X., & Yu, G. (2021). clusterProfiler 4.0: A universal enrichment tool for interpreting omics data. *Innovation (Cambridge (Mass.))*, *2*(3), 100141. https://doi.org/10.1016/j.xinn.2021.100141

Wu, X., & Tu, B. P. (2011). Selective regulation of autophagy by the Iml1-Npr2-Npr3 complex in the absence of nitrogen starvation. *Molecular Biology of the Cell*, *22*(21), 4124–4133. https://doi.org/10.1091/mbc.E11-06-0525

Xiong, W. C., Okano, H., Patel, N. H., Blendy, J. A., & Montell, C. (1994). repo encodes a glial-specific homeo domain protein required in the Drosophila nervous system. *Genes & Development*, *8*(8), 981–994. https://doi.org/10.1101/gad.8.8.981

Yang, M., Wang, H., Chen, C., Zhang, S., Wang, M., Senapati, B., Li, S., Yi, S., Wang, L., Zhang, M., Yin, S., He, Y., Xue, L., Lin, S., & Ho, M. S. (2021). Glia-derived temporal signals orchestrate neurogenesis in the Drosophila mushroom body. *Proceedings of the National Academy of Sciences of the United States of America*, *118*(23), e2020098118. https://doi.org/10.1073/pnas.2020098118

Yu, G. (2018). *enrichplot: Visualization of Functional Enrichment Result*. Bioconductor.